REVIEW

Fabrication for paper-based microfluidic analytical devices and saliva analysis application

Zeji Hao[1] · Hongyu Chen[1] · Xin Shi[1] · Wei Tan[1] · Guorui Zhu[1]

Abstract

Paper-based microfluidic analytical devices (µPADs) have shown great potential in the field of analysis due to their advantages of rapid analysis, environmental friendliness and the ability to realize the flow of fluid without external power. Saliva is an emerging biofluid which is used in diseases diagnostic and screening for the easy collection and the reflection of the physiological state. This review focuses on the fabrication methods for two-dimensional (2D) and three-dimensional (3D) µPADs and their applications on the saliva analysis. In the first part, the flow mechanism in µPADs is discussed. The second part mainly introduces the fabrication methods for the µPADs and compares the different methods. The third part presents the application of µPADs in the detection of biomarkers such as nitrite, glucose, and thiocyanate in saliva. Finally, the research directions of saliva analysis are discussed in the conclusion. There have been a lot of researches on µPADs, but the fabrication methods and applications need to be further studied to meet the commercial needs.

1 Introduction

Miniaturized total analysis systems (µTAS), also known as lab-on-a-chip, were firstly proposed by Manz and Winder (1990). Their significance lies in the control of the fluid on a micron scale, so as to realize the laboratory operations involved in the field of biology and chemistry on a chip of several square centimeters. Compared with traditional laboratory technology, µTAS have the advantages of miniaturization and integration, portability, and are widely used in chemical analysis, clinical detection and food analysis (Bhakta et al. 2014; Sackmann et al. 2014). At present, the main materials of microfluidic chip include monocrystalline silicon, polymethyl methacrylate (PMMA) and polydimethylsiloxane (PDMS) (Duffy et al. 1998; Norouzi et al. 2018). Among them, PDMS occupies a considerable position in the current microfluidic chip manufacture. In 2007, Martinez et al. (2007) achieved the manipulation of liquid flow by building hydrophobic patterns on paper. Since then,

paper has developed rapidly as a cheap alternative material for microfluidic chips. Microfluidic chips based on paper are called paper-based microfluidic analytic devices (µPADs).

Compared with other materials, paper possesses the capillary forces which can pump liquids without external pumping systems. The size of µPADs is relatively compact and, by processing specific channel structure on the paper surface, it can meet many requirements such as quick sample analysis. Now, the combination of microfluidic paper chip and analysis technology is the hotspot of current analysis equipment research. Recently, µPADs have shown great potential in clinical diagnosis by detecting body fluids such as blood (Vella et al. 2012), plasma (Yang et al. 2012), urine (Rossini et al. 2018) and saliva (de Castro et al. 2019). Among these biological fluids, saliva has received more attention because of its convenience of collection and analysis.

Saliva, as a reliable biofluid, is a slightly acidic (pH = 6–7) biological fluid that exists in large quantities in the oral cavity (Humphrey and Williamson 2001; Lee and Wong 2009). It is secreted mainly (90%) by the three major salivary glands including the parotid gland, submandibular gland and sublingual gland, while a small amount (10%) is secreted by the small salivary glands distributed in the oral mucosa (Ilea et al. 2019; Kaczor-Urbanowicz et al. 2017).

✉ Guorui Zhu
  zhuguorui@tju.edu.cn

1 School of Chemical Engineering and Technology, Tianjin University, Tianjin 300350, China

Saliva is mainly composed of water (94–99%), in addition to many organic (protein, glucose, antibody, cytokines) and inorganic biomarkers (nitrogenous products, carbonate, etc.) (Humphrey and Williamson 2001; Zheng et al. 2021). These biomarkers can be used to reflect the oral local and the global health of the body. In addition, the oral cavity contains microbial communities, including bacteria, fungi and viruses. Oral local lesions and general diseases can lead to changes in the oral microbiome (Ilea et al. 2019; Kilian et al. 2016). Therefore, the detection of microorganisms in saliva also has medical value.

Based on the above characteristics, saliva, like blood and urine, can be used as a typical sample for screening and diagnosis of a variety of pathologies. Generally, the collection of blood samples is invasive, which makes patients uncomfortable, and the collection of urine samples is considered an invasion of privacy (Ilea et al. 2019). Compared with other samples, the saliva analysis has the following advantages: saliva collection is easy, does not require specialized medical training and can be performed by ordinary people; thus, it facilitates a simple analysis at home. At the same

time, the simple and convenient collection is non-invasive and friendly for patients, which greatly reduces the anxiety level of patients during sample collection. Healthy adults produce about 0.3–0.4 ml of saliva per minute, so saliva collection overcomes the limited production of samples (urine and tears). Non-invasive collection methods also reduce the risk of cross-contamination to a certain extent (Fernandes et al. 2020; Kaczor-Urbanowicz et al. 2017; Tiwari 2011).

This review aims to depict the fabrication method for two types of structures of μPADs, two dimensions (2D) and three dimensions (3D), and highlights the key advances in saliva analysis (see Fig. 1).

2 Flow mechanism in μPADs

The main driving force of liquid flow in μPADs is capillary force. The hydrophilic surface of paper fiber is conducive to the diffusion of liquid. At present, there are two kinds of flow models for liquid in the paper:
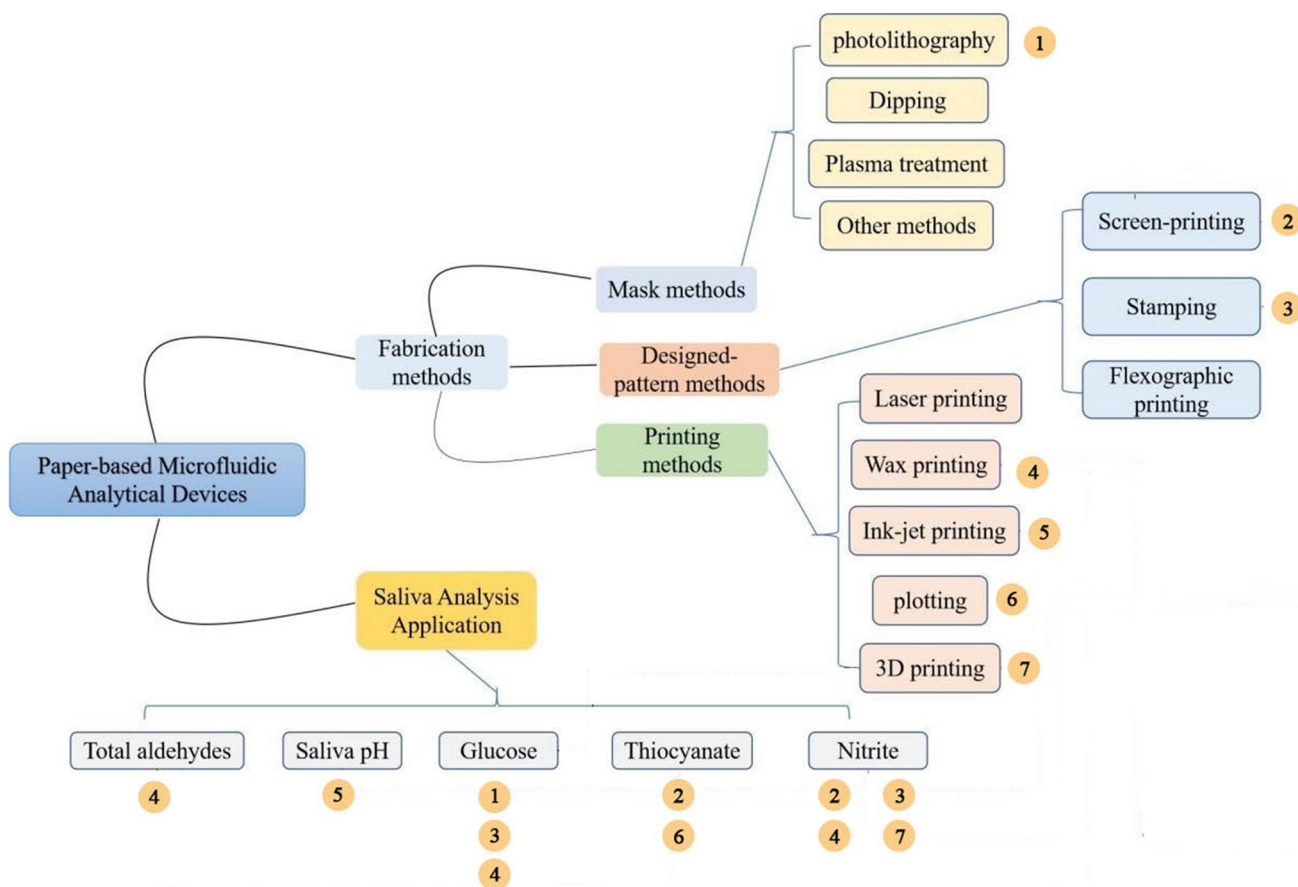

Fig.1 Categories of fabrication of paper-based microfluidic devices and their application in saliva detection; the fabrication methods involved in the saliva analysis application part are numbered. These methods are used to make paper-based microfluidic analytical devices to detect different biomarkers in saliva

Lucas–Washburn equation based on the flow of Poiseuille in capillary tube and Darcy's law which was developed from the phenomena.

When fluids flow in paper, the micrometric pore size of cellulose paper results in Reynolds numbers (Re) lower than 1—the laminar flow, where the viscous forces are dominant. As a result, the flow velocity mostly depends on the equilibrium between the surface tension and viscous resistance.

Generally, we are concerned with the distance traveled by the liquid. Based on $Re < 1$, the distance moved by the liquid front (L_f) in the paper strip can be estimated using the Lucas–Washburn Equation during the wicking process (Washburn 1921):

$$L_f^2 = \frac{\gamma D \cos(\theta)}{4\mu} t, \tag{1}$$

where L_f is the distance traveled by the liquid front within the porous material (paper), D is the pore diameter, t is the permeating time, γ and μ are, respectively, the surface tension and viscosity of the liquid and θ is the contact angle. According to this equation, the distance traveled by the liquid can be increased by improving the surface tension of the liquid. It also shows that the liquid front velocity decreases with time due to viscous resistance. The wicking behavior is often defined as $h \sim t^{1/2}$.

As for Darcy's law, it can be used to calculate the flow rate, which is the part we care about. It is important to note that Darcy's law applies only to incompressible Newtonian liquids. Darcy's law is derived from momentum equation, and it is given as follows (Whitaker 1986):

$$\nabla P = -\frac{\mu}{\kappa} \vec{V}. \tag{2}$$

For one-dimensional lateral flow on paper strips, where the elevation is constant and $Re_p < 1$ (gravity and inertial effects are neglected), Darcy's law reduces to a simple linear relation between the volumetric flow rate Q and gradient of pressure ΔP occurring over the length L of the paper strip (Osborn et al. 2010):

$$Q = -\frac{\kappa A}{\mu L} \Delta P, \tag{3}$$

where κ is the permeability of the paper (in m^2), A is the hydrophilic paper cross-sectional area perpendicular to flow, μ is the dynamic viscosity (Pa s) and ΔP is the pressure drop across the length L, which is the combination of the atmospheric, hydrostatic and capillary pressures.

These two models are helpful in the design of paper chip. By adjusting the paper surface contact angle, the microchannel can achieve effective control of the fluid. In addition, compared with Lucas–Washburn equation which is only for one-dimensional flow, Darcy's law can also be used for two-dimensional or three-dimensional flow modeling (Ahmed et al. 2016).

3 Fabrication methods for µPADs

The surface processing of paper chip is mainly through the partial hydrophilization or hydrophobization of the paper to form a hydrophilic channel. Recently, different fabrication methods and the selection of hydrophobic materials have been developed. In general, these methods can be divided into three categories: (1) mask methods, which require additional masks to assist in manufacturing, such as photolithography, dipping, plasma treatment, vapor phase deposition, wet etching and handheld corona treatment; (2) designed-pattern methods, which do not require additional masks, but require equipment with designed patterns to transfer the patterns to the paper, such as screen printing, stamping and flexographic printing; (3) printing methods, which can directly form the desired pattern on the paper by printing without making masks or corresponding equipment beforehand, such as plotting, wax printing, inkjet printing, laser treatment and 3D printing.

3.1 Mask methods

3.1.1 Photolithography

Photolithography for the fabrication of paper-based chips was originally proposed by Martinez' group (2007). The process of this simple method for patterning paper is shown in Fig. 2. The chromatography paper was soaked in the SU-8 2010 photoresist and baked at 95 ℃ to remove the cyclopentanone in solution. The pre-treated paper was then exposed to ultraviolet light through a mask and followed by a post-bake at the same temperature with the pre-bake to cross-link the exposed part of photoresist. The uncross-linked photoresist was removed by soaking the treated paper in propylene glycol monomethyl ether acetate (PGMEA), and the paper was patterned after washing it with propan-2-ol. For a more rapid and cheaper fabrication, Martinez' group proposed a new method which was called FLASH in 2008 (Martinez et al. 2008a, b). In this method, there was no need for a clean room or special equipment, except a UV lamp and a hot plate. What is more, the fabrication was more convenient. In Kamali's (Kamali et al. 2018) study, they adjusted the process parameters so that PGMEA was no longer used. For the eco-friendly fabrication, SU-8 photoresist was replaced by water-based polyurethane acrylate, which was more environmental friendly and of low cost (Lin et al. 2020). A laser-based method was proposed by Sones (2014). In this study, the UV lamp was replaced by UV laser scanning, so
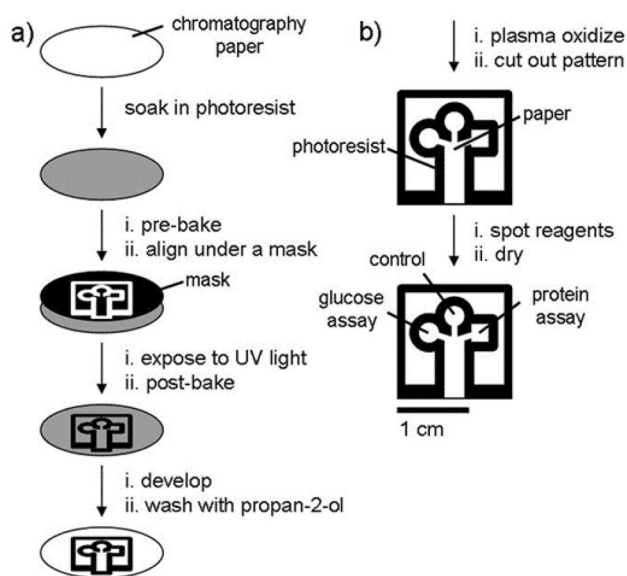
Fig. 2 The method for patterning paper into millimeter-sized channels proposed by Martinez' group (Martinez et al. 2007). **a** Photolithography was used to pattern SU-8 photoresist embedded into paper; **b** the patterned paper was modified for bioassays

the higher-resolution µPADs were obtained without photo masks. The methods mentioned above created physical barriers, which tend to break when the paper was bent. To overcome this problem, some researchers proposed a method, in which the hydrophobic barriers were built by silanization. In

the method, the paper was hydrophobized by impregnation with octadecyltrichlorosilane (OTS) *n*-hexane solution, and hydrophilized by exposure to UV light through the photo mask. (Asano and Shiraishi 2015; Nargang et al. 2018) Based on the photocatalytic property of titanium dioxide, a new method was proposed in 2014 (Songok et al. 2014). The surface of the paper was made hydrophobic by coating the TiO$_2$ particles on the surface. Then the treated paper was exposed to ultraviolet through a photo mask, after which the hydrophilic channels on the surface were built. The µPADs fabricated by photolithography have relatively high resolution, while the fabrication equipment is more expensive than that of other methods.

3.1.2 Dipping

Wax dipping is an easy method for fabrication (Songjaroen et al. 2011, 2012), with the advantages of simplified steps and low cost. In this method, paper and the iron mold which was designed to the desired pattern were held together by a glass slide and a magnet. Then this assembly was dipped into the melted wax for 1 s to transfer the wax into the paper. The paper was patterned after the solidification of wax. High temperature is required in this process to melt wax. Guo et al. (2019a, b) proposed a method which was similar to, but cheaper than wax dipping. The fabrication procedure is depicted in Fig. 3. In this study, the iron mould was replaced by single-sided adhesive tape. The hydrophobic reagent was polystyrene in chloroform instead of wax, so there was no
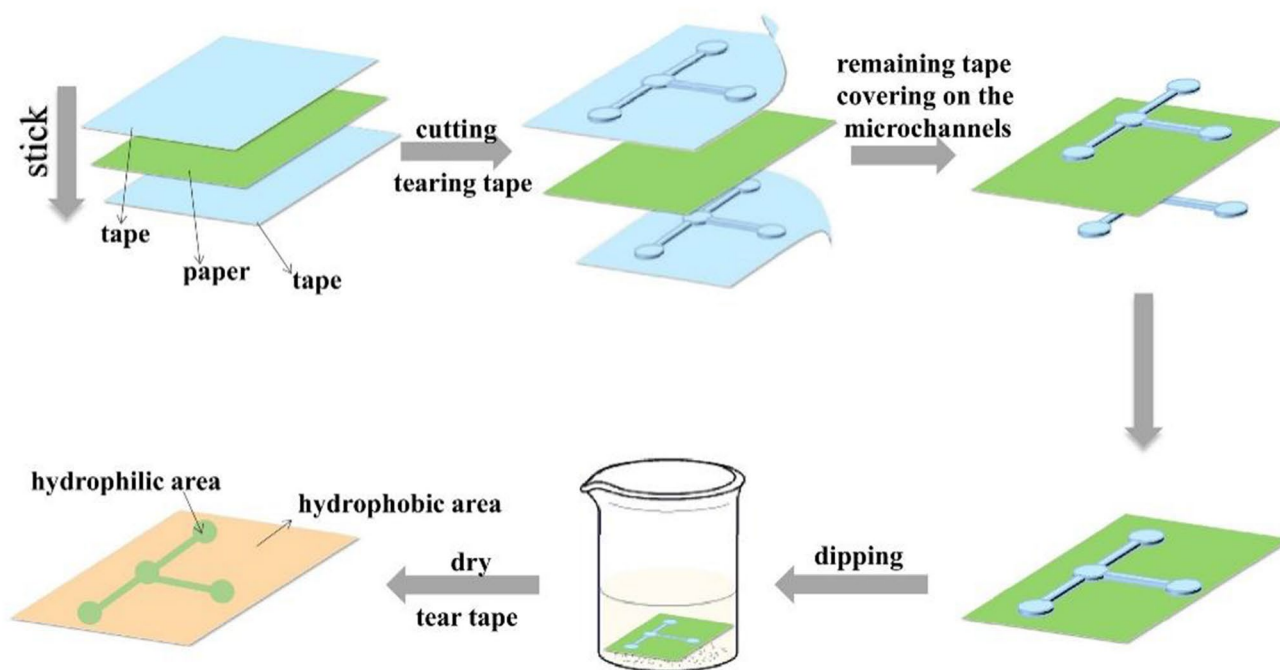

Fig. 3 Schematic diagram of the dipping fabrication procedure in Guo's study (2019a, b)

need for a hot plate to melt wax. Generally, the dipping methods can fabricate μPADs in several minutes and are of low cost.

3.1.3 Plasma treatment

Plasma is the matter that exists in the form of ions and electrons. Basically, it is a gas that has been electrified and charged with freely moving electrons in both the negative and positive state. It carries a good amount of internal energy. When all these molecules, ions and atoms come together and interact with a particular surface, plasma treatment is initiated. Hence, the effects of plasma treatment upon any surface can also be specified or precisely tuned by selecting a gas mixture, pressure, power, etc. Li et al. (2008) used plasma treatment to make microfluidic pattern on the paper surface. The filter paper was hydrophobized by dipping the paper in an alkyl ketene dimer AKD–heptane solution (0.6 g/L) and placing it in a fume cupboard to allow evaporation of heptane. After that, the paper was baked at 100 ℃ for 45 min to cure the AKD. Then, the hydrophobized paper was sandwiched by metal masks with the desired patterns and then placed into a vacuum plasma reactor for 15 s. After these steps, hydrophilic patterns were formed on the paper. The paper can also be hydrophobic patterned by plasma polymerization. In Kao's (2014a, b) study, the paper which was sandwiched by two metal masks was exposed to the plasma to deposit fluorocarbon films. However, the plasma treatment needed more expensive equipment. To overcome this shortcoming, Kao et al. (2014a, b) also developed a portable and flexible air microplasma generation device for fabrication of μPADs. In this method, the materials such as AKD and fluorocarbon are cheap, while the price of equipment falls.

3.1.4 Other methods

Other methods such as vapor phase deposition (Demirel and Babur 2014; Haller et al. 2011; Kwong et al. 2013), wet etching (Cai et al. 2014) and handheld corona treatment (Jiang et al. 2016) were also used for fabrication of μPADs by some researchers. The vapor phase deposition used evacuated sublimation chamber for fabrication. The wet etching which was similar to inkjet etching used the designed mask, not inkjet printer to pattern. These methods are not used widely because of the expensive equipment or multistep processes.

For mask methods, the paper is patterned with a mask made of metals or polymers. The shortcoming of these methods is that different masks need to be processed for different patterns. Thus, mask methods are difficult to apply in mass production of paper chips.

3.2 Designed-pattern methods

3.2.1 Screen printing

Screen printing is a method in which the paper is patterned through a screen. The hydrophobic material penetrated through the mesh in the screen to the paper, thereby forming a hydrophobic patterning in the paper. Therefore, different patterns correspond to different screens. The first hydrophobic material used in screenprinting was wax, so, the method is also called wax screen printing (Dungchai et al. 2011; Ma et al. 2018; Shang et al. 2019; Wang et al. 2012). Figure 4 depicts the fabrication steps for wax screen printing. The solid wax was rubbed through a screen onto the paper to form the patterns on the surface and melted into the paper to form the hydrophobic barriers with a hot plate.

Wax can only be penetrated into the paper when melted, so it is not very convenient on some occasions. Without wax, other hydrophobic materials can also be applied in screen printing. In some studies, the wax was replaced by hydrophobic ink, which could penetrate into the paper without a hot plate (Jarujamrus et al. 2019; Sameenoi et al. 2014; Sitanurak et al. 2019; Teepoo et al. 2019). Jorayu Sitanurak (Sitanurak et al. 2019) used ink as hydrophobic material to fabricate μPADs. The process is shown in Fig. 5. The ink applied through the screen penetrates through the paper, and the patterned paper was ready to use after drying. Currently, these hydrophobic materials included polystyrene, polylactic acid, polyvinyl chloride and *cis*-1,4-polyisoprene. Another method was the combination of screen printing and photolithography (Lamas-Ardisana et al. 2017, 2018). The ultraviolet curable inks penetrated the paper through screen-printing and were then cured in an ultraviolet oven. Jaruwan Mettakoonpitak (Mettakoonpitak et al. 2021) reported the use of simple polycarprolactone (PCL) screen printing for
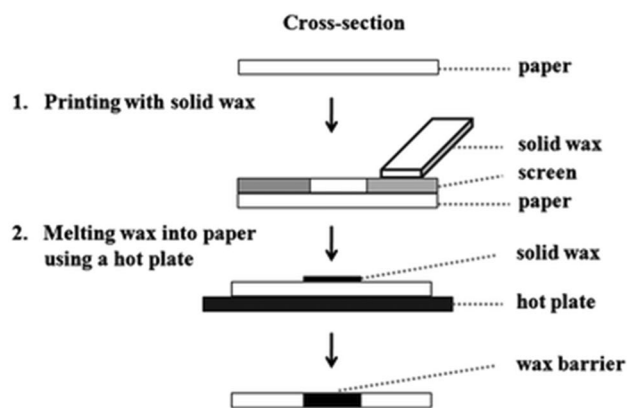
Fig. 4 Schematic diagram of the fabrication step for wax screen-printing method which is mentioned in Wijitar Dungchai's study (Dungchai et al. 2011)
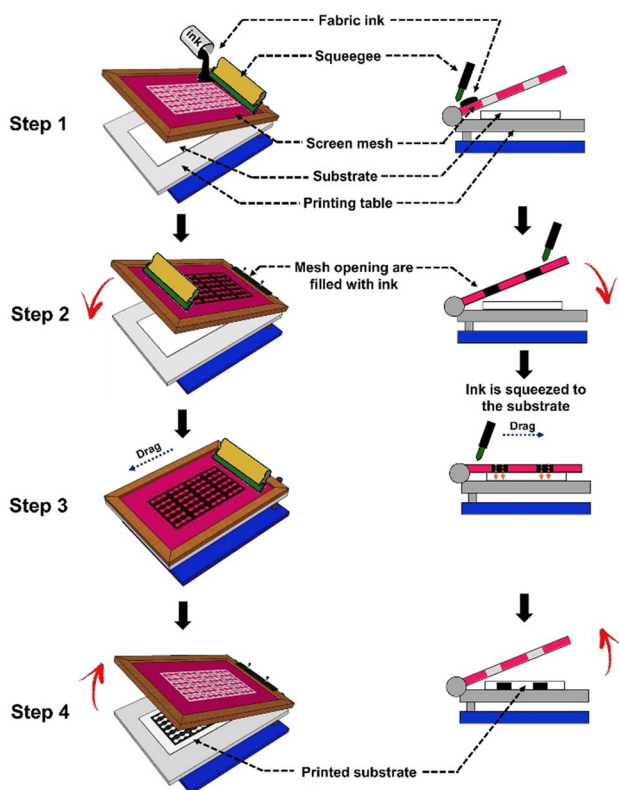
Fig. 5 Schematic diagram of the fabrication step for the screen-printing method proposed by Jirayu Sitanurak's group (Sitanurak et al. 2019). In step 1, the substrate (15 cm×20 cm) is fixed onto the screenprinting table. A mixture of PVC fabric ink and its solvent (total volume∼5 mL) is poured onto the screen mesh. In step 2, a squeegee with a rubber blade is dragged across the mesh to fill all mesh opening. In step 3, the screen mesh now filled with ink is pressed onto the substrate and the squeegee is again dragged from one end to the other end (at a rate of about 2 s/stroke). Steps 2 and 3 are repeated three times. In step 4, the screen is released and the printed substrate is taken out and hung to dry at ambient temperature in a good ventilation environment

µPADs fabrication. The PLC showed low dispersion into paper compared to wax printing, resulting in relatively high resolution. The PCL solution was squeegeed through the screen and penetrated the paper to create 3D hydrophobic barrier. Screenprinting has the advantages of convenience and low cost, but the channel resolution is lower.

3.2.2 Stamping

Like screenprinting, stamping requires different stamps to meet different pattern requirements. Contact stamping has been widely used for simple and fast fabrication (Akyazi et al. 2016; Curto et al. 2013; Duangdeewong et al. 2020; Mathaweesansurn et al. 2020). Arjnarong Mathaweesansurn (2020) proposed a method in which the µPADs for simultaneous multiple-point standard addition assay were fabricated by rubber stamping. The fabrication details are

shown in Fig. 6. With a PDMS-based or rubber stamp and an indelible ink, the paper could be patterned in several seconds by placing the stamp on the paper. The stamp was designed to the desired pattern and the ink was hydrophobic material. The stamping methods are simple and rapid, while the fabrication of stamps is complex in that the different patterned papers need different stamps. Flash foam stamp lithography (He et al. 2014; Yao et al. 2016) and atom stamp (Guan and Sun 2020) were similar methods to get the patterned paper, while the fabrication of stamps was simpler. Another method was the combination of the wax printing and the hot embossing stamp (de Tarso Garcia et al. 2014; Postulka et al. 2019). In this method, the surface of the paper was uniformly covered with a layer of wax. A metallic stamp which was designed with the desired pattern was preheated and then brought in contact with the wax-printed paper to the melted wax. Tansu Golcez (Golcez et al. 2021) used 3D CAD design software to design various stamps and prints with high precision using a 3D printer. The 3D-printed stamp was then mounted onto the base of a self-inking stamp using double-sided tape. The designed stamp was used to cast the resin on a paper towel and filter paper to form hydrophobic channels.

3.2.3 Flexographic printing

Flexographic printing is a method of mass production used in industries. Juuso Olkkonen used flexographic printing to make fluidic structures in paper, and the illustration of this process is shown in Fig. 7 (Olkkonen et al. 2010). In this method, the solution of polystyrene in toluene or in xylene was used as hydrophobic printing ink, and the ink was transferred onto the paper by flexographic printing. PDMS could also be used as printing ink (Hiltunen et al. 2018; Määttänen et al. 2011). Liu et al. (2019) proposed a method in which flexographic printing was used to transfer wax onto paper, and a hot plate was used to melt wax for hydrophobic barriers. These methods have a great advantage than others, in that µPADs can be produced in large quantities by flexographic printing. However, the equipment is relatively expensive, and the preparation for printing is complex. In this method, the paper is patterned by the relief patterns in the printing plate, so different printing patterns require different printing plates.

Similar to the mask methods, the designed-pattern methods also need to pre-manufacture the corresponding equipment to manufacture the different µPADs. However, these methods do not require the mask and paper to be assembled together and can achieve continuous production. Both screenprinting and flexographic printing can realize mass production of µPADs, which have great advantages in factory production of µPADs in the future.

Fig. 6 The fabrication steps of the µPAD by contact stamping are mentioned in Mathaweesansurn's study (Mathaweesansurn et al. 2020). **a** Photograph of the custom-designed stamping device, **b** ink filling, **c** stamping of pattern of the hydrophobic barrier on paper and **d** the final design of the µPAD for the multiple-point standard addition assay
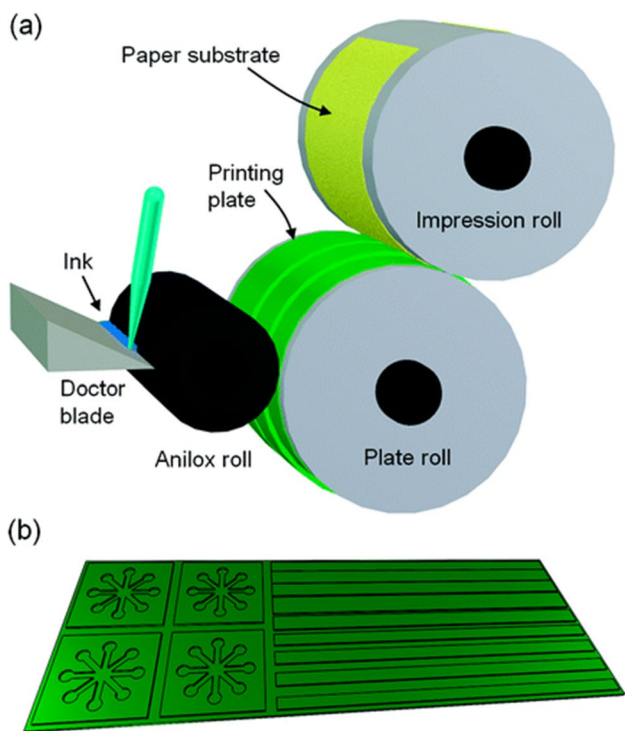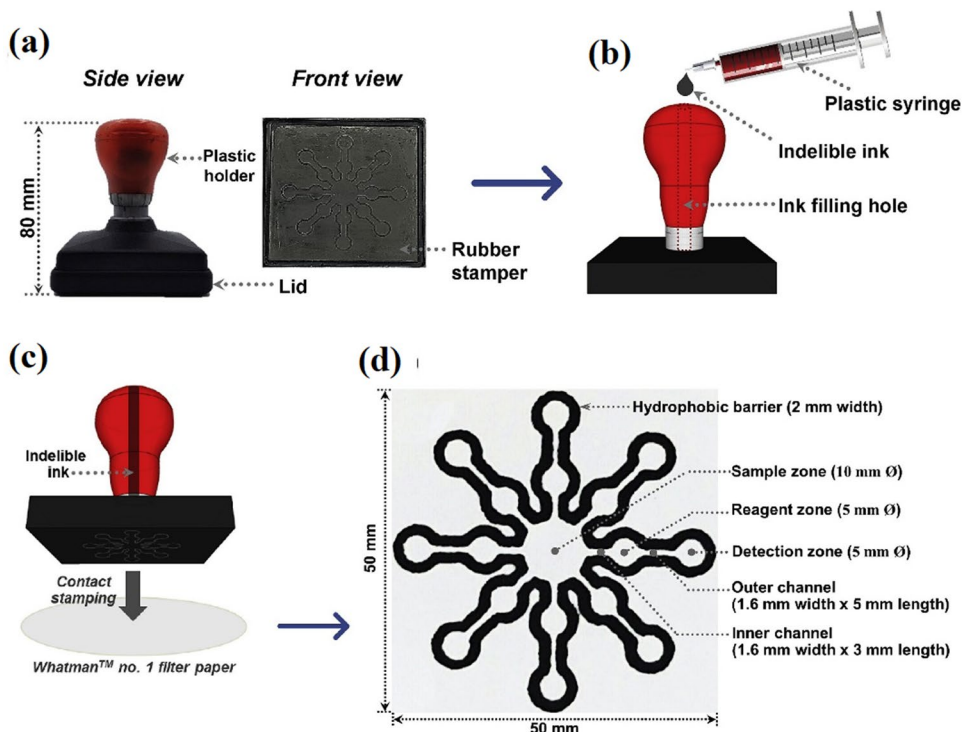

Fig. 7 Schematic illustration of the flexography unit used in Juuso Olkkonen's study (Olkkonen et al. 2010)

3.3 Printing methods

3.3.1 Plotting

Bruzewicz' group proposed a method using the modified *x,y*-plotter for the fabrication of µPADs (Bruzewicz et al. 2008). In the method, the modified plotter printed the solution of PDMS which was hydrophobic onto paper to get patterned paper. The width of the hydrophobic barriers in the patterned paper was similar to 1 mm, but for which the resolution was lower than that of photolithography. However, because PDMS was an elastomer, the printed paper could be bent or folded without destroying the pattern, which was more advanced than photolithography. In some studies, the solution of PDMS was replaced by permanent marker inks, which contained a hydrophobic resin (Amin et al. 2017; Ghaderinezhad et al. 2017). Nie et al. (2012) proposed a one-step method, in which the plotter was replaced by metal templates with specific patterns and the hydrophobic barriers were created by permanent marker inks. Different from other plotting methods, this one-step method belongs to the mask methods. In addition, plotting could be used for the printing electrode arrays on paper for a digital microfluidic chip (Soum et al. 2019). In these plotting methods, the equipment is of low cost and the µPADs are physically flexible devices, while resolution of µPADs is low.

3.3.2 Wax printing

Wax printing is a simple and commercial method which is extensively used (Carrilho et al. 2009; Lei et al. 2015; Preechakasedkit et al. 2018; Rattanarat et al. 2013; Rossini et al. 2021; Trofimchuk et al. 2020; Yehia et al. 2020). It uses a commercially available printer to print patterns of wax on the hydrophilic paper surface, and then the wax is melted into the paper to form complete hydrophobic barriers with thermal treatment. In 2009, Carrilho's group (2009) described a detailed study on wax printing; the operating procedure is depicted in Fig. 8. Ricardo Brito-Pereira (2021) used a printer to print hydrophobic wax on fluorinated polymer membranes. After printing, the samples were placed on a hot plate at 100 °C for 10 min for the wax to penetrate the substrates all the way through to the opposing surface to fabricate the barriers that are able to properly contain the fluids. The wax printing process was rapid, and the material was cheap. However, the utilization of the lower resolution along with the relative high price of wax printer are the main drawbacks of this method.

Wax printing technology has a wide range of applications, not only for making 2D chips, but also involving steps for 3D model fabrication. The method of making two-dimensional patterns with wax printing and then assembling them into a three-dimensional model is called
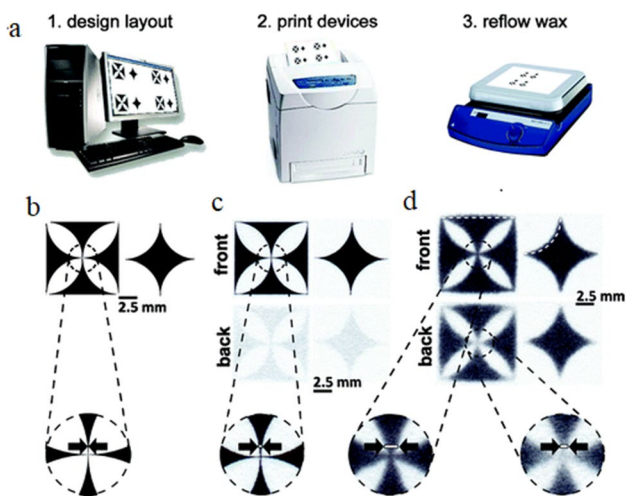

Fig. 8 Patterning hydrophobic barriers in paper by wax printing mentioned in Whiteside's group. (Carrilho et al. 2009). **a** Schematic representation of the basic steps (1–3) required for wax printing. **b** Digital image of a test design. The central area of the design was magnified to show the smaller features. **c** Images of the test design printed on Whatman no. 1 chromatography paper using a solid ink printer. The front and back faces of the paper were imaged using a desktop scanner. d. Images of the test design after heating the paper. The dashed white lines indicate the original edge of the ink. The white bars in the insets highlight the width of the pattern at the position indicated by the arrows (color figure online)

stacking. The use of stacking to fabricate µPADs was first proposed by Martinez' group (Martinez et al. 2008a, b). The fabrication was realized by alternately layering patterned paper and double-sided adhesive tape (Cao et al. 2020; Chun et al. 2014; Im et al. 2016; Li et al. 2019, 2020; Martinez et al. 2008a, b). To realize the vertical flow of the fluid, the hydrophobic double-sided adhesive tape was predrilled and the holes were filled with cellulose powder. However, this method required accurate alignment between the layers; otherwise, the fluid would be blocked in the vertical direction, which was a problem for mass production. Subsequently, Lewis' group (2012) proposed a new method for high-throughput assembly of devices in which the double-sided adhesive tape was replaced by spray adhesive. In this method, only the edges of each layer of paper were aligned, and a large number of devices could be aligned at the same time. Individual devices were obtained by cutting the assembled sheets. However, the spray adhesive had an adverse effect on the wettability of paper. To solve this problem, some researchers showed that the 3D microchannel structures could be built in a single layer of paper (Jeong et al. 2015; Li and Liu 2014). To achieve it, the paper was double-side printed with wax pattern, and the depth of wax penetration was adjusted by controlling the heating condition and the density of printed wax. The number of microchannels could be up to four layers in a single sheet of paper (Li and Liu 2014).

Apart from stacking, some researchers used origami to fabricate 3D µPADs (Ding et al. 2016; Jiang et al. 2019; Jiao et al. 2020; Sechi et al. 2013; Sun et al. 2021). In this method, the paper was patterned by the way of wax printing method and then folded in a pre-designed way without positioning alignment to produce 3D µPADs (Chen et al. 2021). Figure 9 shows a structure of 3D vertical-flow paper-based device proposed by Jiao (2020). Pesaran (2021) described an origami 3D design of a paper-based potentiometric sensor, in which the designed patterns were printed on one side of the filter paper and then the paper layers folded on each other for the integration of different electrodes, in contact with a hydrophilic channel. To prevent the liquid from flowing through the cracks of the paper layers, the folded paper needed to be fixed with clamps (Ding et al. 2016) or pinched by fingers (Choi et al. 2015) for using. On the basis of this method, Chen et al. (Chen et al. 2019) developed a new 3D-µPAD that combined a sliding strip and antibody storage functions on a single sheet of paper to improve the reproducibility and user friendliness of the test, and lower sample consumption. By adopting the sliding strip design, the operation processes could be effectively reduced. However, most of the folding methods needed clamps to maintain the layers close to each other. Moreover, the complex folding relationships were prone to errors.

Fig. 9 The structure of 3D
vertical-flow paper-based
device proposed by Jiao (2020).
a Design and **b** photo of the
paper-based device showing
the size and shape. **c** Photo
of folded paper-based device.
Photos showing the **d** front
and **e** back surface of the 3D
vertical-flow paper-based device
(color figure online)
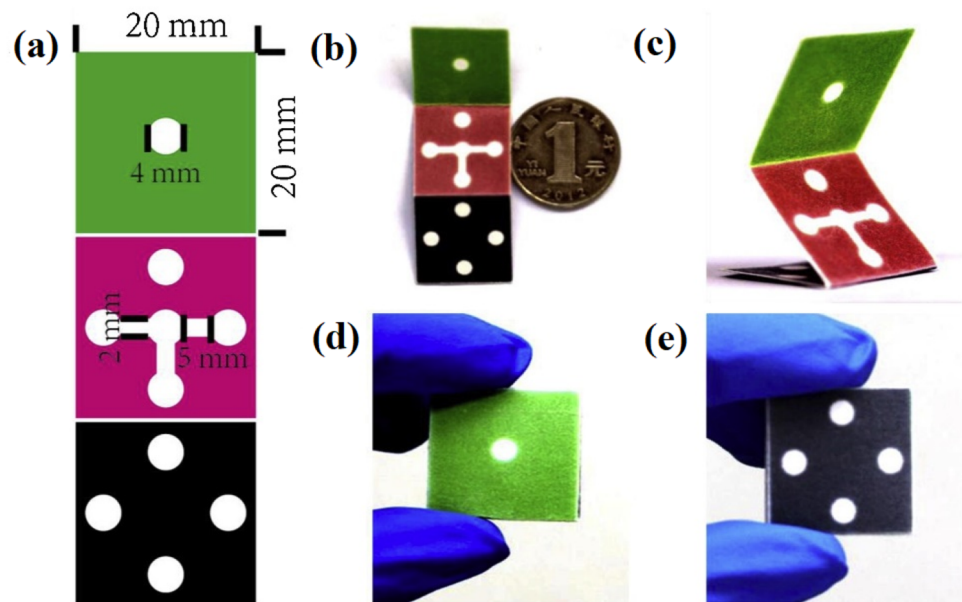
3.3.3 Inkjet printing

Inkjet printing is a method which uses a modified inkjet
printer. In this approach, the ink in the cartridge was
replaced by other hydrophobic materials. By printing the
solution into paper, the paper was patterned. In some stud-
ies (Chakma et al. 2016; Li et al. 2010), the hydrophobic
material was AKD–heptane solution, and the printed paper
was heated at 100 ℃ to cure AKD onto the cellulose fib-
ers. Another method (Henares et al. 2017; Maejima et al.
2013) used the UV-curable ink as the hydrophobic material,
and the printed paper was cured by UV lamp. Jagirdar et al.
(2015) proposed that the ink may be replaced by olive oil
suspended in isopropanol (IPA) and the paper cured in a hot
air oven at 140 ℃. In Le's (2021) study, diethylene glycol
monobutyl ether (DEGBE) was used as solvent-based ink for
the inkjet printing step. Inkjet printing could be also used
to print reagents on the paper (Guo et al., 2019a, b; Ruecha
et al. 2017).

Another method, also called "inkjet etching", is printing
solution onto the hydrophobic paper, to form hydrophilic
channels on the surface of the paper. In Cai's study (2015),
the paper was hydrophobic by soaking in a trimethoxyoc-
tadecylsilane (TMOS)–heptane solution, and the patterned
paper was achieved by printing the NaOH aqueous solu-
tion onto it. In other methods (Abe et al. 2008, 2010), the
paper was soaked in a solution of poly(styrene) in toluene for
hydrophobization, and then the toluene was printed onto the
poly(styrene)-modified paper to dissolve the polymer mate-
rial for patterning. Th whole process is shown in Fig. 10.

The µPADs fabricated by inkjet printing have relatively
high resolution, and it is simple to print with a modified
inkjet printer.

3.3.4 Laser treatment

Chitnis et al. (2011) proposed a fabrication method by
laser treatment. This method was based on paper with a

Fig. 10 Schematic representa-
tion of the fabrication process of
the inkjet-printed microfluidic
multianalyte chemical sensing
paper featuring microfluidic
channels connecting a central
sample inlet area with three
different sensing areas and a
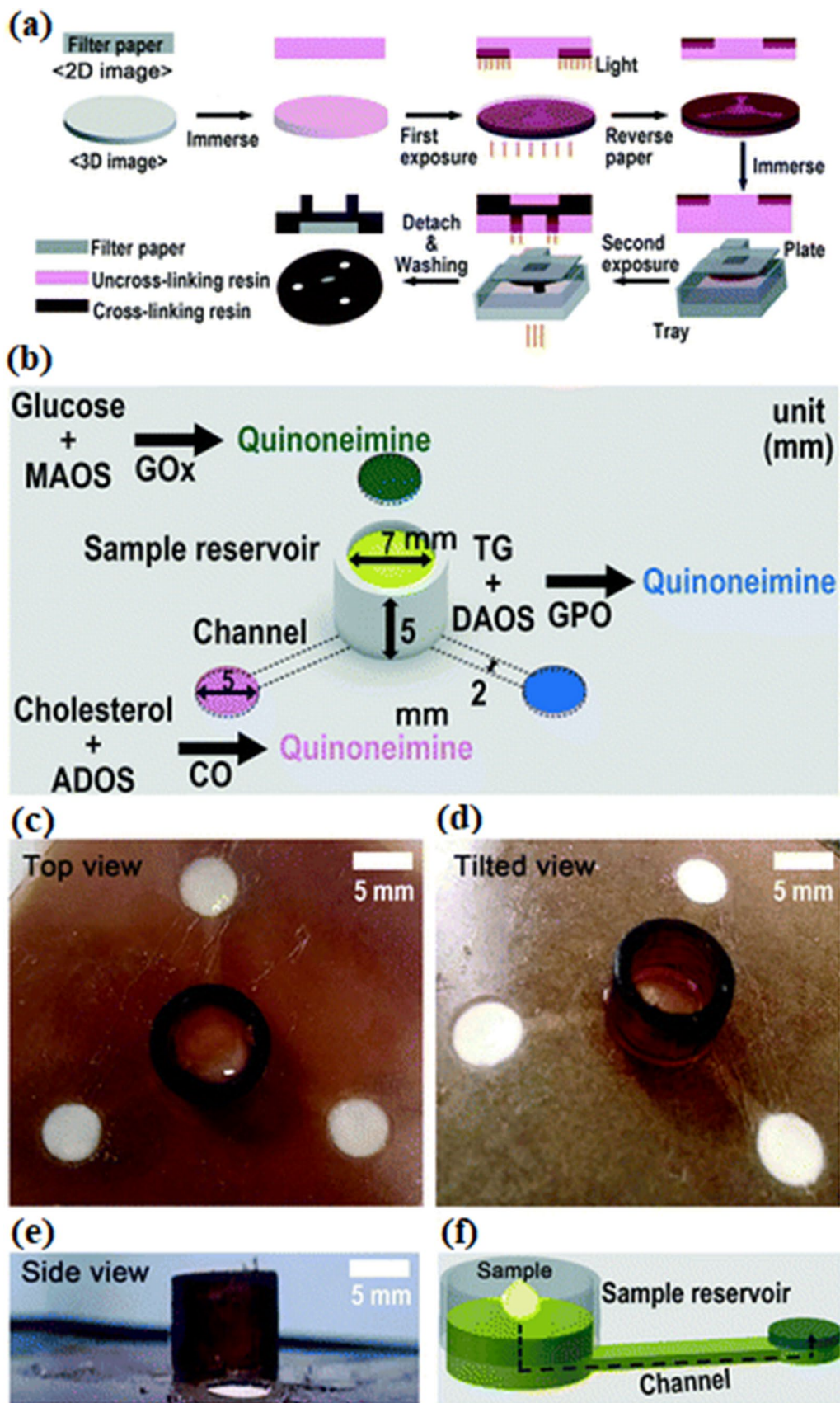reference area (Abe et al. 2008)
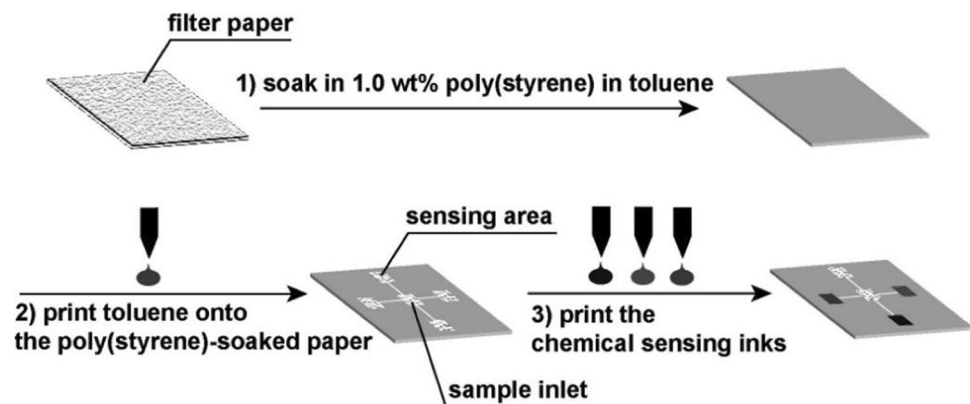
◄**Fig. 11** Printing of the 3D-μPAD for enzymatic detection of multiple analytes proposed in Sungsu Park's study (Park et al. 2018). **a** A schematic describing 3D printing processes for double-sided patterning on the filter paper. **b** A schematic of the 3D-μPAD for simultaneous detection of glucose, cholesterol, and TG. **c** Top view of the 3D-μPAD. **d** Isometric view of the 3D-μPAD. **e** Side view of the 3D-μPAD. **f** A schematic showing the transport of the sample solution from the sample reservoir through the embedded microchannel to the detection zone on the 3D-μPAD

hydrophobic surface coating. It was able to selectively modify the surface structure and property of paper by using a CO_2 laser to create hydrophilic patterns which have higher resolution (62 ± 1 μm) on papers. Ghosh et al. (2019) used a laser printer to print the patterns onto the paper, and the toner ink was melted into the paper by heating the printed paper. μPADs fabricated by laser treatment had high resolution, while the laser was expensive. Zhang et al. (2019) proposed a method which combined laser and wax printing. In this method, the front of the paper was evenly coated with wax in advance, and then a diode laser was used to heat the back side of the paper to melt the wax into the paper, resulting in a patterned paper. Some researchers used CO_2 laser cutting machine to cut the untreated paper, and the hollow microstructures were used as 'hydrophobic barriers' (Modha et al. 2021; Nie et al. 2013). This was a physical method without any chemical process similar to knife plotting (Fenton et al. 2009). The pattern after laser cutting could be used to compose a three-dimensional model. In Xiao's (2019) study, the paper was patterned by laser cutting, and the non-functional zones in the paper were further made hydrophobic with wax. Then these papers which already had patterns were combined together.

3.3.5 3D printing

3D printer which is based on fused deposition modeling (FDM) technology was used for the μPADs fabrication (Puneeth et al. 2019). PCL filament with low melting pointing was used as the printing material for patterning the hydrophobic barriers on paper. In some studies, researchers have used 3D printer to fabricate 2D-μPADs. Chiang et al. (2019) combined the FDM-3D printer with wax printing. In this method, the printing material was wax. The printer can melt wax, so there was no need for external heating. He et al. (2016) used a stereolithography 3D printer for the μPADs fabrication, which was similar to photolithography, as the hydrophobic material is UV resin. Using 3D printer was fast to fabricate μPADs, while the printer was of high cost and the resolution depended on the 3D printers. This method was also a good choice for making 3D-μPADs. Park et al. (2018) reported a fabrication method for 3D-μPADs made of plastics without the need for additional assembly. The production process is shown in Fig. 11. Both sides of

the paper were printed via liquid resin photopolymerization using a digital light processing (DLP) printer. The sample reservoir and detection zones were located on the top of the 3D-μPADs, and three microchannels were located on the bottom. The design could be used to analyze three biomarkers at the same time. The microchannels at the bottom reduced the impact of evaporation on the analysis effect, and the design improved the signal uniformity compared with 2D paper chips. Using DLP-3D printing technology, Fu et al. (2019) realized automatic adhesion and alignment between different layers of paper. It was more advanced than the traditional stacking method.

In this section, we discuss the main fabrication methods of μPADs and analyze their advantages and disadvantages. On the whole, these fabrication methods can be divided into three categories, among which the mask methods and the designed-pattern methods require the corresponding equipment to be manufactured in advance to meet the fabrication requirements of μPADs with different patterns, while the printing methods do not require additional equipment to realize the patterning of paper. Most of the mask methods are cheap and convenient, in that the masks are easy to fabricate. Photolithography also uses masks in making μPADs, but the method is more complex and expensive than others. The μPADs fabricated by photolithography have a high resolution, but the materials involved in the fabricated process are not environmentally friendly, so it is necessary to explore new photoresistors to realize the green production of μ-PADs. Designed-pattern methods have great potential in mass production of μPADs, because of the advantages of fabricating μPADs easily and quickly. However, the resolution of μPADs produced by these methods is low, so improving the resolution is very important. The printing methods can realize paper patterning directly, so it is simpler in operation. Wax printing, which is a mature manufacturing method ,is relatively more used at present. The commercial wax printer can realize a relatively fast production of μPADs, and the resolution of the μ-PADs fabricated by wax printing can generally meet the application needs. 3D printing has the advantage of digital production and can realize rapid production. However, the resolution of μPADs obtained by this method is also low, so new printing materials need to be developed to improve the resolution. The paper fiber is modified by AKD solution in inkjet printing method, and the μPADs are flexible. Also, the modified inkjet printer has poor compatibility with the material, so a special inkjet printer has to be developed for the production of μPADs. There are some shortcomings in the current methods, so it is necessary to develop a method that can meet the requirements of rapid fabrication and high resolution, for example the combination of photolithography and flexographic printing. The summary of fabrication methods is shown in Table 1.

Table 1 Summary of fabrication methods for µPADs

Categories	Fabrication methods	Equipment	Reagents (hydrophobic material)	Advantages	Limitations	References
Mask methods	Photolithography	Lithography equipment, mask, hot plate; UV lamp	PGMEA, polyurethane acrylate, OTS	High resolution	Expensive equipment and reagents, complex steps	(Kamali et al. 2018; Lin et al. 2020; Martinez et al. 2007; Martinez et al. 2008a, b; Nargang et al. 2018; Sones et al. 2014; Songok et al. 2014)
	Dipping	Iron masks, glass slide, magnet; single-sided adhesive tape masks	Wax; polystyrene	Low cost, fast and simple fabrication	Low resolution	(Guo et al., 2019a, b; Songjaroen et al. 2011, 2012)
	Plasma treatment	vacuum plasma reactor, metal masks, fume cupboard, oven; microplasma generation device	AKD; fluorocarbon	The reagents (AKD and fluorocarbon) are relatively cheap	Expensive equipment	(Kao and Hsu, 2014a, b; Li et al. 2008)
	Vapor phase deposition	Deposition equipment, masks, handheld UV lamp	Poly(o-nitrobenzyl methacrylate); poly(chloro-p-xylene)	Simple steps	Expensive equipment	(Demirel and Babur 2014; Haller et al. 2011; Kwong et al. 2013)
	Wet etching	Paper mask, glass slide, heater	TMOS, NaOH	Quick fabrication	Low resolution, difficulty in mass production	(Cai et al. 2014)
	Handheld corona treatment	Handheld corona generator, plastic mask	OTS	Simplicity in operation, low in cost	Multisteps, difficulty in mass production	(Jiang et al. 2016)
Designed-pattern methods	Screen printing	Screen printer, squeegee, hot plate; ultraviolet oven	Wax; polystyrene; polylactic acid; polyvinyl chloride; cis-1,4-polyisoprene; ultraviolet curable inks; PCL	Low cost, simple fabrication steps	Relatively low resolution	(Dungchai et al. 2011; Jarujamrus et al. 2019; Lamas-Ardisana et al. 2017, 2018; Ma et al. 2018; Mettakoonpitak et al. 2021; Sameenoi et al. 2014; Shang et al. 2019; Sitanurak et al. 2019; Teepoo et al. 2019; Wang et al. 2012)
	Stamping	PDMS, metallic, flash foam or 3D-printed stamp	Wax; PDMS; commercial ink	Low cost, simple fabrication steps	Low resolution	(Akyazi et al. 2016; Curto et al. 2013; de Tarso Garcia et al. 2014; Duangdeewong et al. 2020; Golcez et al. 2021; Guan and Sun 2020; He et al. 2014; Mathaweesansurn et al. 2020; Postulka et al. 2019; Yao et al. 2016)
	Flexographic printing	Customized printing equipment, hot plate	Polystyrene, PDMS, wax	Fast and accessible to mass production	High cost, requires complex preparation and cleaning	(Hiltunen et al. 2018; Liu et al. 2019; Määttänen et al. 2011; Olkkonen et al. 2010)

Table 1 (continued)

Printing methods						
Plotting	X,y-plotter	PDMS, marker inks	Low cost	Low resolution	(Amin et al. 2017; Bruzewicz et al. 2008; Ghaderinezhad et al. 2017)
Wax printing	Wax printer, hot plate	wax	Simple and fast fabrication, Mature commercialization	Relatively low resolution, the heating step	(Brito-Pereira et al. 2021; Carrilho et al. 2009; Lei et al. 2015; Preechakasedkit et al. 2018; Rattanarat et al. 2013; Trofimchuk et al. 2020; Yehia et al. 2020)
Inkjet printing	modified inkjet printer, oven, UV lamp	AKD; UV-curable ink; olive oil; DEGBE; TMOS, NaOH; poly(styrene), toluene	High resolution, simple fabrication	Requires customized inkjet printers	(Abe et al. 2008; Cai et al. 2015; Chakma et al. 2016; Henares et al. 2017; Jagirdar et al. 2015; Le et al. 2021; Li et al. 2010; Maejima et al. 2013)
Laser treatment	CO$_2$ laser cutting machine	Parchment paper, SiO$_2$; wax	High resolution, simple to fabrication	Expensive equipment	(Chitnis et al. 2011; Ghosh et al. 2019; Nie et al. 2013; Zhang et al. 2019)
3D printing	3D printer	Wax, UV resin, PCL	Fast and accessible to mass production	Expensive equipment	(Chiang et al. 2019; He et al. 2016; Park et al. 2018; Puneeth et al. 2019)

Those methods discussed above can be used in making both 2D and 3D models. The 2D µPADs realize the flow of fluid in the plane range, thus achieving relatively simple detection. However, they cannot realize multistep detection. 3D µPADs mainly have multilayer structure, which can realize the lateral and vertical flow of liquid. On this basis, more complex channel structures and reaction zones can be designed on the same footprint, so as to realize multistep reaction detection and reduce sample volume. At present, there are more related studies to improve the detection of µPADs. 3D-µPADs produced by 3D printing need to further explore the diversity of structural design to meet more functional requirements. All in all, 2D and 3D-µPADs have great potential for analysis and detection, but it is necessary to develop cheap, simple and relatively high-resolution production methods to meet the needs of commercial production.

4 The application of µPADs for analysis of saliva

µPADs is low cost, compact and convenient to operate, so the fabrication of these models opened up the possibility to develop miniaturized lab-on-a-chip platforms capable of detecting biomarkers. In this section, µPADs used in detecting different types of biomarkers (nitrite, thiocyanate, glucose, total aldehydes, PH value and reductase) in saliva are discussed. The current limitations of saliva analysis are also proposed.

4.1 Nitrite

Nitrite in saliva is a potential biomarker for oral cancer and periodontal disease. In general, the detection of nitrite is based on the colorimetric reaction of Griess reaction which promotes the formation of a magenta azo compound. At present, some groups used different fabrication methods to manufacture µPADs for quantitative detection of nitrite in saliva. Bhakta et al. (2014) used wax printing to create a hydrophobic barrier in the paper, so as to realize the directional flow of liquid. Fig. 12a shows the design of this µPAD. The µPADs consisted of a main channel, four identical arms, four uptake zones and four test zones to separate components in the Griess reagent and reduce the degradation of the reagent during storage. After fabrication of the µPADs, Griess reagent was spotted on the testing zones. For the analysis procedure, sample or standard solution was dispensed onto a hydrophobic material. The main channel of the µPAD was then brought into vertical contact with the droplet to allow sample uptake by capillarity and drive the solution into the branched channels and testing zones. In addition, the acetic acid in

the reagent was replaced with 5% H_3PO_4 to maximize the color development. On the basis of these modifications, the accuracy of nitrite detection is improved. The device was used to detect nitrite with a limit of detection (LOD) 10 µmol L^{-1} and a detection range of 10–1000 µmol L^{-1}. de Castro et al. (2019) manufactured µPADs by craft cutter printing and this chip could quantitatively detect nitrite and glucose. The device depicted in Fig. 12b was designed to contain two detection zones and one sampling zone for colorimetric assays, and it could be assembled into the silicone mouth guard using a 3D-printed holder toward wearable paper-based devices. The holder to assemble µPADs was fabricated using a 3D printer with FDM technology and ABS polymeric filament. Two pieces were manufactured to be used as base and cover, allowing to keep µPADs enclosed. The paper tip was kept outside the holder to allow saliva absorption on the paper surface and, consequently, it was transport under lateral flow along the channels toward detection zones. Nitrite colorimetric assay was performed through the modified Griess reaction in which the LOD value was 7 µmol L^{-1}, and the limit of quantification (LOQ) value was 25 µmol L^{-1}. Cardoso et al. (2015) used a stamping-based method to form paraffin barrier in paper to develop µPADs. In this method, the paraffin was transferred from a paraffined paper to the native paper by a preheated metal stamp. The flower-shaped µPADs were designed in a geometry containing eight circular detection zones for bioassays interconnected by microfluidic channels and one central zone to the sample inlet. The Griess reaction was modified by replacing the sulfanilic acid by sulfanilamide and hydrochloric acid. Hence, the reaction was faster and the color was more stable than the original Griess reaction. Jiang et al. (2016) produced hydrophilic channels in hydrophobic paper treated with octadecyl trichlorosilane (OTS) by corona treatment, thus producing µPADs for nitrite detection. A flower-shaped channel network with eight detection zones shown in Fig. 12c was chosen as the device designed to perform multisample assays simultaneously and under the same condition. Chiang et al. (2019) used a mask-free 3D wax printing method to build paper chips for nitrite detection. The device had a central reservoir, six uniformly distributed hydrophilic channels and six circular detection zone, in which the standard nitrite solutions with different concentrations to be tested can be added at the same time. Sitanurak et al. (2019) used screen printing to fabricate µPADs for nitrite detection. T-shirt screen ink as a novel material for rapid fabrication of hydrophobic was used in this study. The production of the µPADs was reasonably high with up to 77 devices per screening (for single layer µPADs). An example of a fabric ink-printed paper substrate is shown in Fig. 12d. This device was applied for the simultaneous quantitation of thiocyanate and nitrite in synthetic saliva.
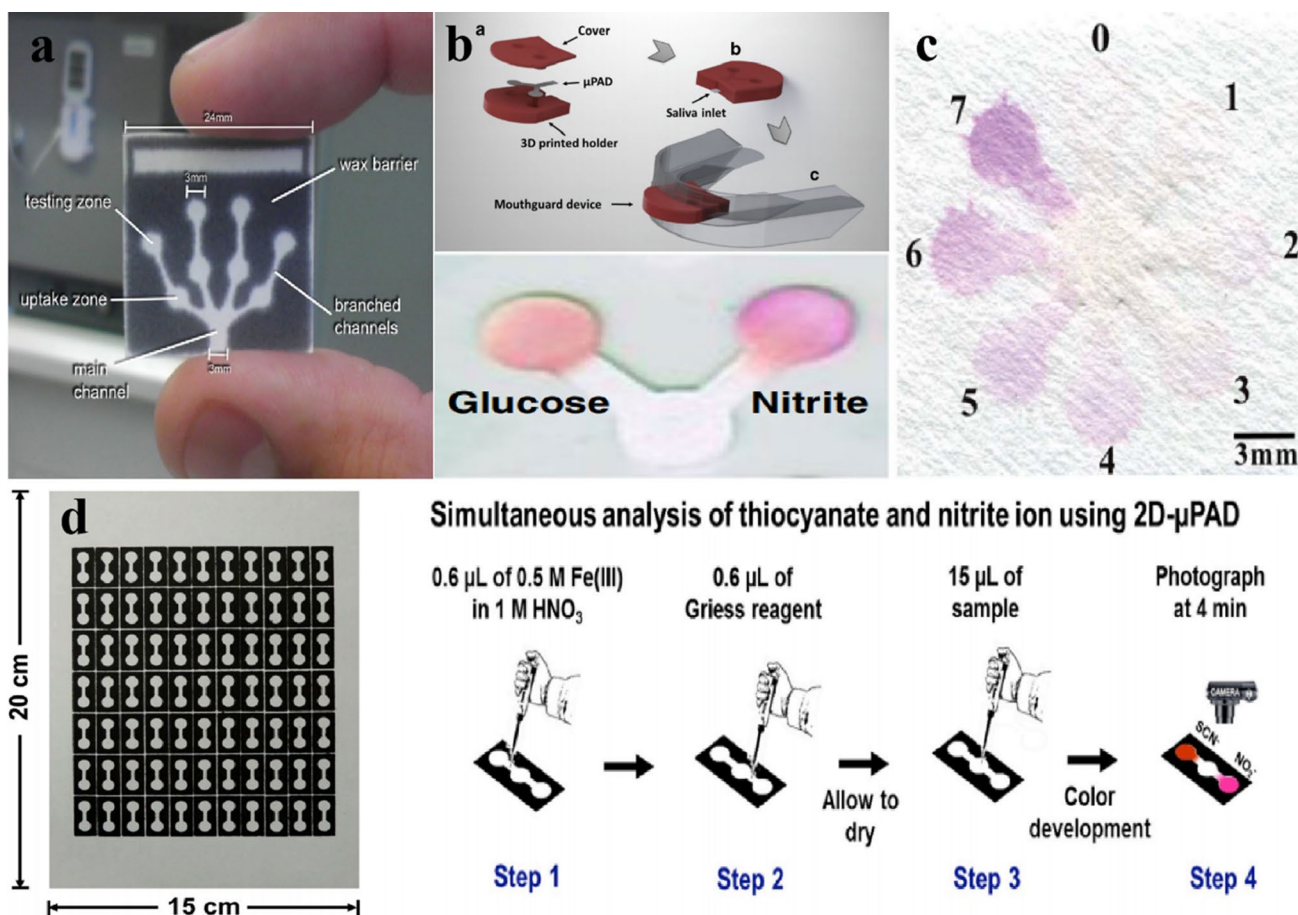
Fig. 12 a The redesigned μPADs for nitrite detection in saliva showing the hydrophilic main channel, branched channels, uptake zones, and testing zones surrounded by the hydrophobic wax barrier (Bhakta et al. 2014). **b** The design of μPADs and the assembling of the μPAD into the mouth guard using a 3D-printed holder toward wearable paper-based devices (de Castro et al. 2019). **c** Scanned image of a color-developed μPAD (Jiang et al. 2016). **d** Example of fabric ink-printed paper substrate showing 77 dumbbell-shaped devices per production, and operating procedures for simultaneous determination of thiocyanate and nitrite in synthetic saliva (Sitanurak et al. 2019).

4.2 Thiocyanate

Thiocyanate is an important biomarker for tobacco smoke exposure and the levels of thiocyanate in saliva can be used to identify smokers and non-smokers. It can be found at different concentration levels in body fluids, and is significantly more concentrated in human saliva. Thiocyanates can react with ferric ions under acidic conditions to form an iron(III)–thiocyanate colored complex. Based on this reaction, thiocyanates can be quantified by analyzing the chromogenic degree of the complex.

For the quantification of thiocyanate, Pena-Pereira et al. (2016) used a one-step plotting method to fabricate μPADs. A stencil containing repeated units of specific dimensions(6 × 6 mm each) was placed under a piece of Whatman filter paper, and the detection areas were easily plotted by using a commercially available permanent marker. The credit card-sized device contained 40 separated test zones.

In the research, the detection method relied on the implementation of a complexation reaction between thiocyanate and iron(III) under acidic conditions. The LOD was 0.06 mmol L^{-1}, the LOQ was 0.21 mmol L^{-1} and the average thiocyanate levels for non-smokers and smokers were in the ranges of 0.28–0.87 mmol L^{-1} and 0.78–4.28 mmol L^{-1}, respectively. Pungjunun (2021) proposed a microcapillary grooved paper-based analytical device being capable of dual-mode sensing (colorimetric and electrochemical detection) for analysis of SCN^- in thiocyanate. A hollow capillary channel was constructed via laser engraved micropatterning functions as a micropump to facilitate viscous fluidic transport. The μpumpPAD which had colorimetric detection zone and electrochemical detection zone is shown in Fig. 13a. For high levels of SCN^-, after applying a working solution or a real sample onto the sample zone, the solution was rapidly wicked along the straight channel through the hollow capillary and then reached the colorimetric detection
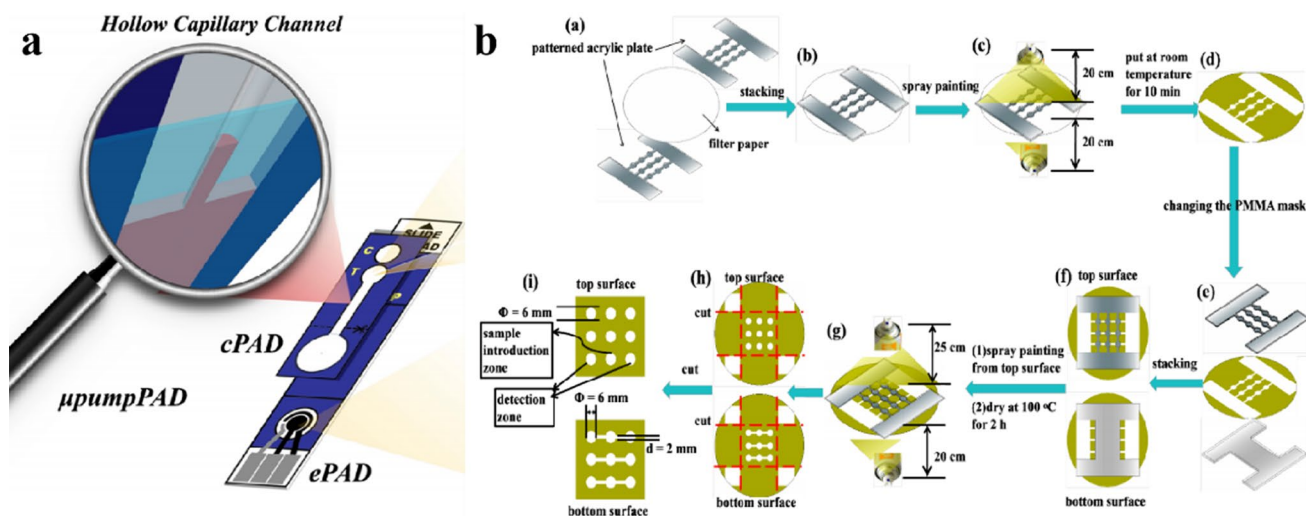
Fig. 13 a Schematic illustration of the hollow capillary channel of the µpumpPAD for dual-mode sensing via colorimetric detection on cPAD and electrochemical detection on ePAD (Pungjunun et al.

2021). **b** The spraying prototyping process for fabricating the 3D sl-µPADs (Yu et al. 2020)

zone. Rapid visible color change could be seen in the color testing zone. However, a low amount of SCN^- could not sufficiently produce observable signals in colorimetric. For low level of SCN^-, µpumpPAD could easily detect the trace level via an electrochemical mode (square wave voltammetry). For the colorimetric detection, in addition to iron (III) and nitric acid, hexadecyltrimethylammonium bromide (CATB) was added to the detection zone to reduce the viscosity of the saliva sample, and polyacrylic acid (PA) was also added to stabilize the colorimetric product. For the electrochemical detection, CATB was added as an additive to enhance the current signal. Yu et al. (2020) used spraying technique to fabricate the three-dimensional single-layered paper-based microfluidic analytical devices (3D sl-µPADs) for the colorimetric detection of nitrite and thiocyanate at the same time. The spraying prototyping process for fabricating the 3D sl-µPADs is illustrated and shown in Fig. 13b. The detection reservoirs on the left were used for nitrite assay and the detection reservoirs on the right were used for thiocyanate detection. At first, the µPAD was prepared by first adding PA to all the assay reservoirs, waiting for 10 min for drying at RT. After that, Griess reagent solution was pipetted to the left detection reservoirs, Fe(III) reagent solution was pipetted to the right detection reservoirs, and then the simultaneous detection of both NO_2^- and SCN^- was performed. A total of the standard containing two anions was pipetted into the central reservoirs for introducing the sample.

4.3 Glucose

Glucose in saliva is a biomarker for diabetes mellitus. Rapid detection of glucose in saliva using µPADs is of

great significance for the treatment of diabetes mellitus. In general, the detection of glucose is achieved by a bienzymatic assay containing glucose oxidase (GOx) and horseradish peroxidase (HRP). The H_2O_2 produced in the reaction reacts with I^{-1} or 3, 3', 5, 5'-tetramethylbenzidine (TMB) and thus causes a color change. The color depth is proportional to the glucose concentration. Chiang et al. (2019) reported an improved method for patterning filter paper by wax printing in a single step in which the hydrophobic wax barrier could be developed without the use of either mask or external heating device. To detect multiple analytes simultaneously under the same conditions, the µPADs were fabricated with a central fluid reservoir and six circular detection zones interconnected each other through the hydrophilic microchannels. Glucose was detected by a bienzymatic assay, and the chromogenic agent was NaI. Jia et al. (2018) used a photolithography method to fabricate the µPADs, and the graphene oxide (GO) was deposited on the surface of the paper to enhance the colorimetric assay performance. There were two types of paper-based microfluidic designs in general, the reservoir array-based design and the lateral-flow design. In this paper, both design strategies were incorporated to this portable system to verify the effectiveness of this device. Figure 14a shows the design and fabrication method of the µPADs. The dispersed GO solution was first pipetted to the µPADs detection zones and allowed to dry, then chromogenic substrate (15 mmol L^{-1} TMB) and the mixture of enzymatic solutions (GOx and HRP) were added to the detection zones in two independent steps. After that, glucose solution with predetermined concentrations was applied to the µPADs. A back camera of a smartphone
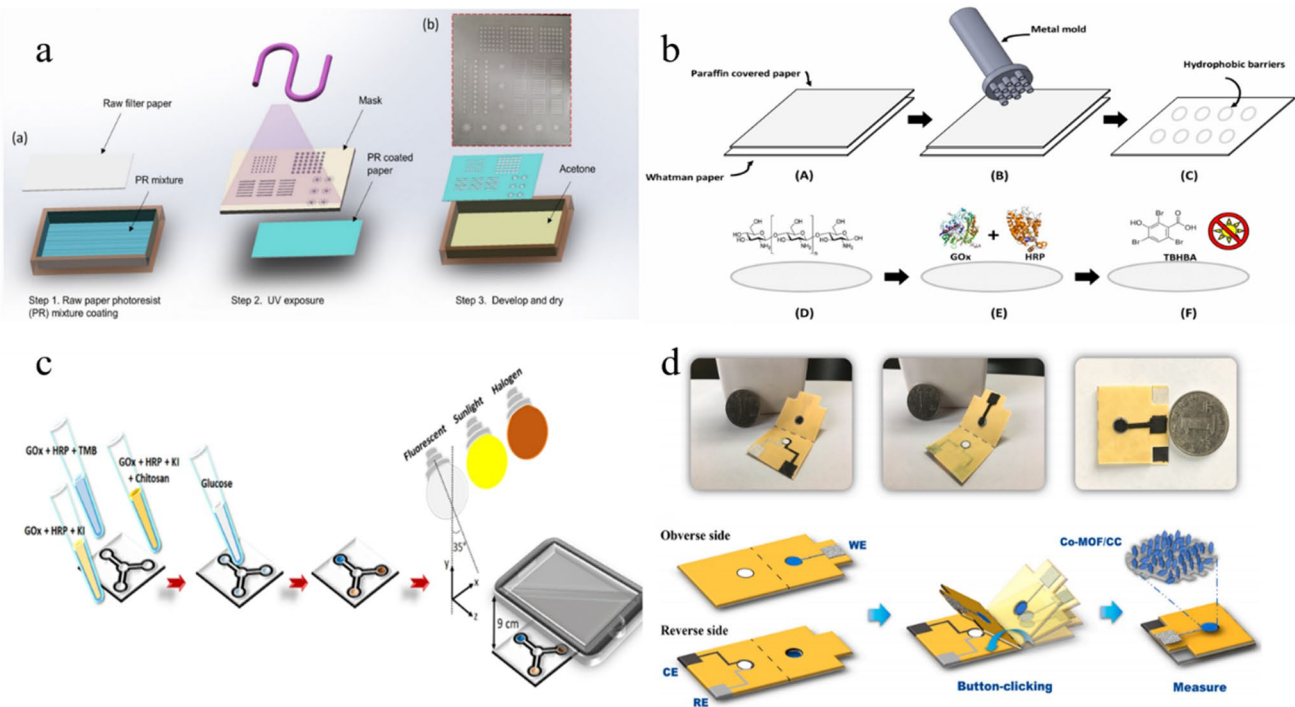
Fig. 14 a Schematic representation of the paper-based sensor fabrication (Jia et al. 2018). **b** Schematic representation of the paper-based sensor fabrication (Santana-Jimenez et al. 2018). **c** Schematic illustration of the glucose determination strategy (Mercan et al. 2021). The change in color in the detection zones of the µPAD is imaged using a smartphone camera under various combinations of fluorescent, halogen and sunlight sources. **d** Photographs of button sensor and 3D schematic of the assay procedure (Wei et al. 2021).

with a fixed focus distance and the 'always on' flash mode was used to take assay images for 60 s after the chip loading. Some researchers have attempted to improve the colorimetric readout by modifying µpads PADs with chitosan (de Castro et al. 2019; Santana-Jimenez et al. 2018). Santana-Jimenez et al. (2018) presented a bienzymatic paper-based sensor suitable for the naked eye detection of glucose in saliva samples. The sensor was obtained by a stamping procedure and modified with chitosan to improve the colorimetric readout. Figure 14b shows the fabrication of the paper-based sensor. During the detection, glucose solution was directly applied to the detection zone, the visual readout was perceived by the naked eye and registered with an office scanner to evaluate the analytical performance. de Castro et al. (2019) fabricated the µPADs by craft cutter printing and combined the µPADs with a mouth guard, so as to realize the real-time detection of glucose in saliva. They also impregnated chitosan solution on the µPADs' surface to enhance the glucose colorimetric assay performance. Mercan (2021) developed a portable platform in cooperating a µPAD with a machine learning to quantify glucose concentration in saliva. The µPADs which had three detection zones were made by wax printing. The detection zones of the µPAD were modified with three different detection mixtures; after the

color change, the images of µPADs were taken with different smartphones under different illumination conditions. Then machine learning was used to classify these images to result in a more adaptive platform against illumination variation and camera optics. The determination strategy is shown in Fig. 14c.

Some researchers tried to detect the glucose with an electrochemical method. Wei (2021) proposed a cobalt metal–organic framework modified carbon cloth/paper (Co-MOF/CC/paper) hybrid button-sensor which was developed as a portable and user-friendly electrochemical analytical chip for nonenzymatic quantitative detection of glucose. Cobalt-MOF moderately crystalized on the CC at ambient state and assembled with the patterned paper electrode to form a hybrid button sensor. The design of the device is shown in Fig. 14d. The fabrication process combined wax printing with origami, while Co-MOF/CC was glued on chip for constructing a three-electrode system, and the final 3D devices could meet the needs of mutistep reaction. The electrochemical performance of Co-MOF/CC/paper hybrid button sensor was investigated by electrochemical impedance spectroscopy (EIS), cyclic voltammetry (CV). For the quantitative detection of glucose, amperometric response was measured in 0.1 mol NaOH (20 µL) at the constant potential of 0.45 V over 50 s for a saturation current.

4.4 Total aldehydes

Total aldehydes in saliva can be used to assess oral cancer risk in that the formaldehyde and acetaldehyde have been linked to cancer risk. Ramdzan's group (Ramdzan et al. 2016) proposed the development of the µPADs for the determination of salivary aldehydes using a colorimetric method involving the reaction between 3-methyl-2- benzothiazolinone hydrazone (MBTH), iron (III) and aldehydes. In their approach, the µPADs were fabricated by the wax printing method and designed to be 3D µPADs with two overlapping paper layers (Fig. 15), so that the reaction sequence could be met. The first layer comprised 15 circular detection zones impregnated with 8 µL of MBTH. The second layer contained 15 reagent zones, and 2 µL of iron(III) chloride were added to each of the second layer zones after the addition of sample to the detection zones in the first layer. Due to the two-step nature of the analytical reaction, the two paper layers were separated by a cellulose acetate interleaving sheet to allow the reaction between the aldehydes in the saliva sample with MBTH to form azine, followed by a blue colored reaction between the azine and the MBTH oxidized by iron(III) after the removal of the interleaving sheet. The detection range of the µPADs for aldehydes was 20.4–114.0 µmol L^{-1}, and the LOD was 6.1 µmol L^{-1}.

4.5 Saliva PH value and reductase

Saliva PH value and reductase are important biomarkers to determine whether dental caries occurs. Dental caries is more likely to occur in a locally acidic environment, and the reductase is not the original ingredient in saliva, but is produced by microbes in the mouth that cause caries. Jagirdar et al. (2015) developed a detection method based on colorimetric analysis for simultaneous measurement of saliva PH value and reductase. The designed device which had a sample zone, a pH detection zone and a reductase detection zone is shown in Fig. 16. In this study, the PH was measured by using a mixture of bromothymol blue and bromocresol green, and the reductase was measured by diazoresorcinol which changed from blue to pink in the presence of

reductase. The µPADs were fabricated by an inkjet printing method, in which the ink was replaced by olive oil. The two tests were combined to give users a more specific understanding of oral health.

4.6 Other biomarkers

In addition to µPADs for small molecule detection, there were some sophisticated paper-based analysis devices for the detection of dengue-specific immunoglobulins (IgG) (Zhang et al. 2015) and the extraction of DNA (Gan et al. 2014; Tang et al. 2017) in saliva. The researchers used the conventional ELISA to validate the dengue IgG-positivity and -negativity in saliva. The result indicated that the test was valid. However, the quantitative analysis of immunoglobulin in saliva still needs further research. The researchers made a simple attempt for the extraction of DNA from saliva, but a more effective analysis method was still needed.

This section summarizes the recent advances in the application of saliva analysis and provides a brief assessment of the commercial potential of the applications, as shown in Table 2. Although these studies demonstrate the potential of µPADs, the characteristics of saliva limit its further development. First, the complex oral environment leads to changes in the composition of collected saliva, which affects the results of biomarkers' detection. In the current studies, most researchers use artificial saliva instead of real saliva to ensure the accuracy of experimental results. Also, some researchers use real saliva for research (Cardoso et al. 2015; Ramdzan et al. 2016). To make sure the results are accurate, the volunteers were asked to rinse their mouth with deionized water before saliva collection. Second, the current detection is still limited to small molecules in saliva, and most biomarkers are detected by colorimetric analysis, so it is still necessary to develop macromolecule detection methods based on the µPADs platform. The most important point is that the concentrations of biomarkers in saliva are several orders of magnitude lower than in serum, which limits the accuracy of biomarker detection, and this limitation puts higher requirements on detection methods.

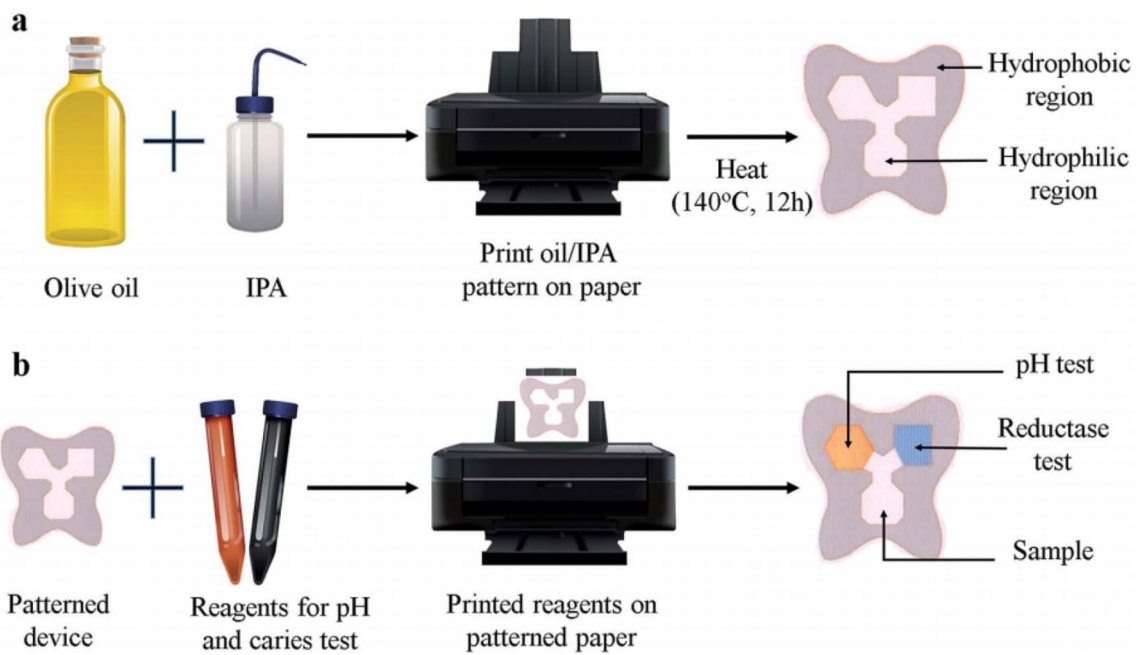**Fig. 15** 3D µPADs design with two layers (Ramdzan et al. 2016)
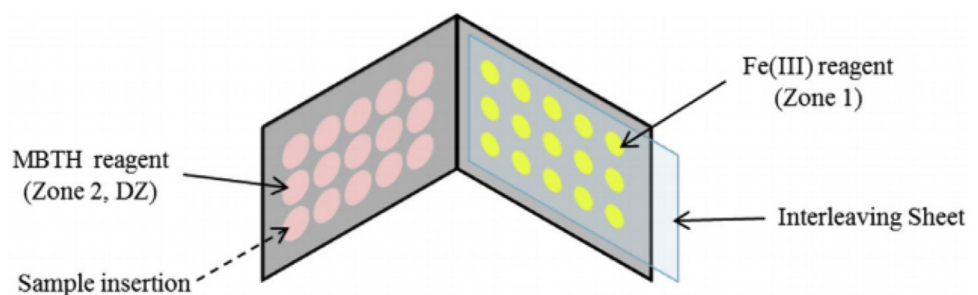
Fig. 16 Process flow for patterning hydrophobic regions on paper and printing dental assay reagents. After printing and curing the hydrophobic barrier, diazoresorcinol (blue square) and pH indicator (yellow hexagon) solutions were printed in specific reaction zones. When saliva was added to the device, it reacted with the assay reagents and resulted in a color change in the designated areas (Jagirdar et al. 2015) (color figure online)

Table 2 Summary of biomarker detection

Biomarkers	Detection mechanism	Reaction or reagents	LOD/LQD	Competitivity	References
Nitrite	Colorimetric	1.Modified Griess reaction (the acetic acid is replaced by 5% H_3PO_4)	10 µmol L^{-1}/	Medium	(Bhakta et al. 2014)
		2. Modified Griess reaction (the acetic acid is replaced by citric acid)	7 µmol L^{-1}/25 µmol L^{-1}	Relatively high	(de Castro et al. 2019)
Thiocyanate	Colorimetric	Iron (III), HNO_3	0.06 mmol L^{-1}/0.21 mmol L^{-1}	Medium	(Pena-Pereira et al. 2016)
		Iron (III), HNO_3/3D µPADs	0.074 mmol L^{-1}/0.25 mmol L^{-1}	Relatively high	(Yu et al. 2020)
	Colorimetric and electrochemical	Iron (III), HNO_3, CATB, PA; CATB	0.2 mmol L^{-1}/0.6 mmol L^{-1} 0.006 mmol L^{-1}/0.02 mmol L^{-1}	High	(Pungjunun et al. 2021)
Glucose	Colorimetric	1. Traditional bienzymatic assay	0.3 mmol L^{-1}/	Low	(Chiang et al. 2019)
		2.Modified bienzymatic assay (GO enhancement)	0.02 mmol L^{-1}/	Relatively high	(Jia et al. 2018)
		3. Modified bienzymatic assay (chitosan enhancement)	0.027 mmol L^{-1}/0.09 mmol L^{-1}	Relatively high	(de Castro et al. 2019)
	Electrochemical	Co-MOF/CC/paper sensor	0.15 mmol L^{-1}/	Relatively high	(Wei et al. 2021)
Total aldehydes	Colorimetric	MBTH, iron (III) and aldehydes	6.1 µmol L^{-1}/20.4 µmol L^{-1}	Medium	(Ramdzan et al. 2016)
PH value	Colorimetric	Bromothymol blue and bromocresol green		Low	(Jagirdar et al. 2015)
Reductase	Colorimetric	Diazoresorcinol		Low	(Jagirdar et al. 2015)

5 Conclusion and outlook

Compared with other microfluidic chips, µPADs have the advantages of low cost and simple operation steps. The fluid flows in the device do not need external equipment, like pump. Passive fluid flow can be achieved in µPADs because of the capillary phenomenon. In this review, we summarize the flow mechanism in the paper, the fabrication methods of 2D and 3D µPADs and the applications of µPADs for analysis of saliva. The fabrication methods for µPADs are divided into three categories, and each of them has their own advantages and disadvantages. Wax is more widely used for the hydrophobic barriers in that there is already a wax printer available for commercial use. However, patterns printed on wax do not have high resolution. These methods mentioned above can not only make 2D chips, but also be used in 3D chips fabrication. 3D µPADs can realize the vertical flow of liquid, which have great potential in realizing the complex flow of liquid. For 3D µPADs, new structures can be developed to meet the requirements of more complex and multistep analysis. Saliva testing plays an important role in the field of POCT, because saliva contains many biomarkers and can be collected non-invasively. This review summarizes the application of saliva analysis based on paper-based microfluidic platform such as the detection of nitrite, thiocyanate and glucose, and points out the prospect of real-time saliva detection. However, as pointed out in Sect. 4, there are still many deficiencies in the current research. Further research is needed on how to realize the application of paper-based microfluidic in limited medical areas and family situations.

Although a variety of manufacturing methods have been proposed, the device produced is not robust enough; hence, the structure is easy to be destroyed during the testing process. In future research, the robustness of the device can be improved by improving the manufacturing method or improving the material properties.

To increase the commercial value of the device, it is necessary to develop manufacturing methods that can achieve mass production, such as combining flexographic printing with wax printing. It is also necessary to improve the detection sensitivity of current detectable biomarkers. In addition, to reduce the influence of complex oral environment on the analysis results, the saliva sample collection procedure should be standardized, such as requiring the sampled person to gargle before sampling.

For the detection of biological macromolecules such as proteins, more effective detection methods are needed, and higher requirements are also put forward for the structure of the devices. The 3D µPADs can realize the complex flow of liquid in the device, which provides a structural basis for multistep reactions. Therefore, relevant structures can be further designed to meet the requirements of different detection methods. At the same time, the electrochemical analysis method and other methods can be combined with the devices to improve the sensitivity of the device analysis.

References

Abe K, Suzuki K, Citterio D (2008) Inkjet-printed microfluidic multi-analyte chemical sensing paper. Anal Chem 80:6928–6934. https://doi.org/10.1021/ac800604v

Abe K, Kotera K, Suzuki K, Citterio D (2010) Inkjet-printed paper-fluidic immuno-chemical sensing device. Anal Bioanal Chem 398:885–893. https://doi.org/10.1007/s00216-010-4011-2

Ahmed S, Bui MP, Abbas A (2016) Paper-based chemical and biological sensors: engineering aspects. Biosens Bioelectron 77:249–263. https://doi.org/10.1016/j.bios.2015.09.038

Akyazi T, Saez J, Elizalde J, Benito-Lopez F (2016) Fluidic flow delay by ionogel passive pumps in microfluidic paper-based analytical devices. Sens Actuators, B Chem 233:402–408. https://doi.org/10.1016/j.snb.2016.04.116

Amin R, Ghaderinezhad F, Li L, Lepowsky E, Yenilmez B, Knowlton S, Tasoglu S (2017) Continuous-ink, multiplexed pen-plotter approach for low-cost, high-throughput fabrication of paper-based microfluidics. Anal Chem 89:6351–6357. https://doi.org/10.1021/acs.analchem.7b01418

Asano H, Shiraishi Y (2015) Development of paper-based microfluidic analytical device for iron assay using photomask printed with 3D printer for fabrication of hydrophilic and hydrophobic zones on paper by photolithography. Anal Chim Acta 883:55–60. https://doi.org/10.1016/j.aca.2015.04.014

Bhakta SA, Borba R, Taba M Jr, Garcia CD, Carrilho E (2014) Determination of nitrite in saliva using microfluidic paper-based analytical devices. Anal Chim Acta 809:117–122. https://doi.org/10.1016/j.aca.2013.11.044

Brito-Pereira R, Macedo AS, Tubio CR, Lanceros-Mendez S, Cardoso VF (2021) Fluorinated polymer membranes as advanced substrates for portable analytical systems and their proof of concept for colorimetric bioassays. ACS Appl Mater Interfaces 13:18065–18076. https://doi.org/10.1021/acsami.1c00227

Bruzewicz DA, Reches M, Whitesides GM (2008) Low-cost printing of poly(dimethylsiloxane) barriers to define microchannels in paper.pdf. Anal Chem 80:3387–3392. https://doi.org/10.1021/ac702605a

Cai L, Xu C, Lin S, Luo J, Wu M, Yang F (2014) A simple paper-based sensor fabricated by selective wet etching of silanized filter paper using a paper mask. Biomicrofluidics 8:056504. https://doi.org/10.1063/1.4898096

Cai L, Zhong M, Li H, Xu C, Yuan B (2015) Defining microchannels and valves on a hydrophobic paper by low-cost inkjet printing of aqueous or weak organic solutions. Biomicrofluidics 9:046503. https://doi.org/10.1063/1.4928127

Cao L, Han GC, Xiao H, Chen Z, Fang C (2020) A novel 3D paper-based microfluidic electrochemical glucose biosensor based on rGO-TEPA/PB sensitive film. Anal Chim Acta 1096:34–43. https://doi.org/10.1016/j.aca.2019.10.049

Cardoso TMG, Garcia PT, Coltro WKT (2015) Colorimetric determination of nitrite in clinical, food and environmental samples using microfluidic devices stamped in paper platforms. Anal Methods 7:7311–7317. https://doi.org/10.1039/c5ay00466g

Carrilho E, Martinez AW, Whitesides GM (2009) Understanding wax printing: a simple micropatterning process for paper-based microfluidics. Anal Chem 81:7091–7095. https://doi.org/10.1021/ac901071p

Chakma B, Jain P, Singh NK, Goswami P (2016) Development of an indicator displacement based detection of malaria targeting HRP-II as biomarker for application in point-of-care settings. Anal Chem 88:10316–10321. https://doi.org/10.1021/acs.analchem.6b03315

Chen CA, Yeh WS, Tsai TT, Li YD, Chen CF (2019) Three-dimensional origami paper-based device for portable immunoassay applications. Lab Chip 19:598–607. https://doi.org/10.1039/c8lc01255e

Chen C-A, Yuan H, Chen C-W, Chien Y-S, Sheng W-H, Chen C-F (2021) An electricity- and instrument-free infectious disease sensor based on a 3D origami paper-based analytical device. Lab Chip. https://doi.org/10.1039/d1lc00079a

Chiang CK, Kurniawan A, Kao CY, Wang MJ (2019) Single step and mask-free 3D wax printing of microfluidic paper-based analytical devices for glucose and nitrite assays. Talanta 194:837–845. https://doi.org/10.1016/j.talanta.2018.10.104

Chitnis G, Ding Z, Chang CL, Savran CA, Ziaie B (2011) Laser-treated hydrophobic paper: an inexpensive microfluidic platform. Lab Chip 11:1161–1165. https://doi.org/10.1039/c0lc00512f

Choi S, Kim S-K, Lee G-J, Park H-K (2015) Paper-based 3D microfluidic device for multiple bioassays. Sens Actuators B Chem 219:245–250. https://doi.org/10.1016/j.snb.2015.05.035

Chun HJ, Park YM, Han YD, Jang YH, Yoon HC (2014) Paper-based glucose biosensing system utilizing a smartphone as a signal reader. BioChip J 8:218–226. https://doi.org/10.1007/s13206-014-8308-7

Curto VF, Lopez-Ruiz N, Capitan-Vallvey LF, Palma AJ, Benito-Lopez F, Diamond D (2013) Fast prototyping of paper-based microfluidic devices by contact stamping using indelible ink. RSC Adv. https://doi.org/10.1039/c3ra43825b

de Castro LF, de Freitas SV, Duarte LC, de Souza JAC, Paixao T, Coltro WKT (2019) Salivary diagnostics on paper microfluidic devices and their use as wearable sensors for glucose monitoring. Anal Bioanal Chem 411:4919–4928. https://doi.org/10.1007/s00216-019-01788-0

de Tarso GP, Garcia Cardoso TM, Garcia CD, Carrilho E, Tomazelli Coltro WK (2014) A handheld stamping process to fabricate microfluidic paper-based analytical devices with chemically modified surface for clinical assays. RSC Adv 4:37637–37644. https://doi.org/10.1039/c4ra07112c

Demirel G, Babur E (2014) Vapor-phase deposition of polymers as a simple and versatile technique to generate paper-based microfluidic platforms for bioassay applications. Analyst 139:2326–2331. https://doi.org/10.1039/c4an00022f

Ding J, Li B, Chen L, Qin W (2016) A three-dimensional origami paper-based device for potentiometric biosensing. Angew Chem Int Ed Engl 55:13033–13037. https://doi.org/10.1002/anie.201606268

Duangdeewong C, Sitanurak J, Wilairat P, Nacapricha D, Teerasong S (2020) Microfluidic paper-based analytical device for convenient use in measurement of iodate in table salt and irrigation water. Microchem J. https://doi.org/10.1016/j.microc.2019.104447

Duffy DC, McDonald JC, Schueller OJ, Whitesides GM (1998) Rapid prototyping of microfluidic systems in poly(dimethylsiloxane). Anal Chem 70:4974–4984. https://doi.org/10.1021/ac980656z

Dungchai W, Chailapakul O, Henry CS (2011) A low-cost, simple, and rapid fabrication method for paper-based microfluidics using wax screen-printing. Analyst 136:77–82. https://doi.org/10.1039/c0an00406e

Fenton EM, Mascarenas MR, Lopez GP, Sibbett SS (2009) Multiplex lateral-flow test strips fabricated by two-dimensional shaping.

ACS Appl Mater Interfaces 1:124–129. https://doi.org/10.1021/am800043z

Fernandes LL, Pacheco VB, Borges L et al (2020) Saliva in the diagnosis of COVID-19: a review and new research directions. J Dent Res 99:1435–1443. https://doi.org/10.1177/0022034520960070

Fu X, Xia B, Ji B, Lei S, Zhou Y (2019) Flow controllable three-dimensional paper-based microfluidic analytical devices fabricated by 3D printing technology. Anal Chim Acta 1065:64–70. https://doi.org/10.1016/j.aca.2019.02.046

Gan W, Zhuang B, Zhang P, Han J, Li CX, Liu P (2014) A filter paper-based microdevice for low-cost, rapid, and automated DNA extraction and amplification from diverse sample types. Lab Chip 14:3719–3728. https://doi.org/10.1039/c4lc00686k

Ghaderinezhad F, Amin R, Temirel M, Yenilmez B, Wentworth A, Tasoglu S (2017) High-throughput rapid-prototyping of low-cost paper-based microfluidics. Sci Rep 7:3553. https://doi.org/10.1038/s41598-017-02931-6

Ghosh R, Gopalakrishnan S, Savitha R, Renganathan T, Pushpavanam S (2019) Fabrication of laser printed microfluidic paper-based analytical devices (LP-microPADs) for point-of-care applications. Sci Rep 9:7896. https://doi.org/10.1038/s41598-019-44455-1

Golcez T, Kilic V, Sen M (2021) A portable smartphone-based platform with an offline image-processing tool for the rapid paper-based colorimetric detection of glucose in artificial saliva. Anal Sci 37:561–567. https://doi.org/10.2116/analsci.20P262

Guan Y, Sun B (2020) Detection and extraction of heavy metal ions using paper-based analytical devices fabricated via atom stamp printing. Microsyst Nanoeng. https://doi.org/10.1038/s41378-019-0123-9

Guo X, Chen Y, Zhang L, Liu W (2019a) An inkjet printing paper-based immunodevice for fluorescence determination of immunoglobulin G. Anal Methods 11:3452–3459. https://doi.org/10.1039/c9ay00893d

Guo X, Guo Y, Liu W, Chen Y, Chu W (2019b) Fabrication of paper-based microfluidic device by recycling foamed plastic and the application for multiplexed measurement of biomarkers. Spectrochim Acta A Mol Biomol Spectrosc 223:117341. https://doi.org/10.1016/j.saa.2019.117341

Haller PD, Flowers CA, Gupta M (2011) Three-dimensional patterning of porous materials using vapor phase polymerization. Soft Matter. https://doi.org/10.1039/c0sm01214a

He Y, Wu Y, Xiao X, Fu J, Xue G (2014) A low-cost and rapid microfluidic paper-based analytical device fabrication method: flash foam stamp lithography. RSC Adv 4:63860–63865. https://doi.org/10.1039/c4ra11150h

He Y, Gao Q, Wu WB, Nie J, Fu JZ (2016) 3D printed paper-based microfluidic analytical devices. Micromach (basel). https://doi.org/10.3390/mi7070108

Henares TG, Yamada K, Takaki S, Suzuki K, Citterio D (2017) "Drop-slip" bulk sample flow on fully inkjet-printed microfluidic paper-based analytical device. Sens Actuators B Chem 244:1129–1137. https://doi.org/10.1016/j.snb.2017.01.088

Hiltunen J, Liedert C, Hiltunen M et al (2018) Roll-to-roll fabrication of integrated PDMS-paper microfluidics for nucleic acid amplification. Lab Chip 18:1552–1559. https://doi.org/10.1039/c8lc00269j

Humphrey SP, Williamson RT (2001) A review of saliva: normal composition, flow, and function. J Prosthet Dent 85:162–169. https://doi.org/10.1067/mpr.2001.113778

Ilea A, Andrei V, Feurdean CN et al (2019) Saliva, a magic biofluid available for multilevel assessment and a mirror of general health-A systematic review. Biosensors (basel). https://doi.org/10.3390/bios9010027

Im SH, Kim KR, Park YM, Yoon JH, Hong JW, Yoon HC (2016) An animal cell culture monitoring system using a

smartphone-mountable paper-based analytical device. Sens Actuators B Chem 229:166–173. https://doi.org/10.1016/j.snb.2016.01.121

Jagirdar A, Shetty P, Satti S, Garg S, Paul D (2015) A paperfluidic device for dental applications using a novel patterning technique. Anal Methods 7:1293–1299. https://doi.org/10.1039/c4ay02802c

Jarujamrus P, Meelapsom R, Naksen P et al (2019) Screen-printed microfluidic paper-based analytical device (muPAD) as a barcode sensor for magnesium detection using rubber latex waste as a novel hydrophobic reagent. Anal Chim Acta 1082:66–77. https://doi.org/10.1016/j.aca.2019.06.058

Jeong SG, Lee SH, Choi CH, Kim J, Lee CS (2015) Toward instrument-free digital measurements: a three-dimensional microfluidic device fabricated in a single sheet of paper by double-sided printing and lamination. Lab Chip 15:1188–1194. https://doi.org/10.1039/c4lc01382d

Jia Y, Sun H, Li X, Sun D, Hu T, Xiang N, Ni Z (2018) Paper-based graphene oxide biosensor coupled with smartphone for the quantification of glucose in oral fluid. Biomed Microdevices 20:89. https://doi.org/10.1007/s10544-018-0332-2

Jiang Y, Hao Z, He Q, Chen H (2016) A simple method for fabrication of microfluidic paper-based analytical devices and on-device fluid control with a portable corona generator. RSC Adv 6:2888–2894. https://doi.org/10.1039/c5ra23470k

Jiang D, Ge P, Wang L et al (2019) A novel electrochemical mast cell-based paper biosensor for the rapid detection of milk allergen casein. Biosens Bioelectron 130:299–306. https://doi.org/10.1016/j.bios.2019.01.050

Jiao Y, Du C, Zong L et al (2020) 3D vertical-flow paper-based device for simultaneous detection of multiple cancer biomarkers by fluorescent immunoassay. Sens Actuators B Chem. https://doi.org/10.1016/j.snb.2019.127239

Kaczor-Urbanowicz KE, Martin Carreras-Presas C, Aro K, Tu M, Garcia-Godoy F, Wong DT (2017) Saliva diagnostics—current views and directions. Exp Biol Med (maywood) 242:459–472. https://doi.org/10.1177/1535370216681550

Kamali B, Asiaei S, Beigzadeh B, Ali Ebadi A (2018) Micro-lithography on paper, surface process modifications for biomedical performance enhancement. Colloids Surf A 555:389–396. https://doi.org/10.1016/j.colsurfa.2018.06.053

Kao P-K, Hsu C-C (2014a) One-step rapid fabrication of paper-based microfluidic devices using fluorocarbon plasma polymerization. Microfluid Nanofluid 16:811–818. https://doi.org/10.1007/s10404-014-1347-5

Kao PK, Hsu CC (2014b) Battery-operated, portable, and flexible air microplasma generation device for fabrication of microfluidic paper-based analytical devices on demand. Anal Chem 86:8757–8762. https://doi.org/10.1021/ac501945q

Kilian M, Chapple IL, Hannig M et al (2016) The oral microbiome—an update for oral healthcare professionals. Br Dent J 221:657–666. https://doi.org/10.1038/sj.bdj.2016.865

Kwong P, Seidel S, Gupta M (2013) Solventless fabrication of porous-on-porous materials. ACS Appl Mater Interfaces 5:9714–9718. https://doi.org/10.1021/am402775r

Lamas-Ardisana PJ, Casuso P, Fernandez-Gauna I et al (2017) Disposable electrochemical paper-based devices fully fabricated by screen-printing technique. Electrochem Commun 75:25–28. https://doi.org/10.1016/j.elecom.2016.11.015

Lamas-Ardisana PJ, Martinez-Paredes G, Anorga L, Grande HJ (2018) Glucose biosensor based on disposable electrochemical paper-based transducers fully fabricated by screen-printing. Biosens Bioelectron 109:8–12. https://doi.org/10.1016/j.bios.2018.02.061

Le NN, Phan HCT, Dang DMT, Dang CM (2021) Fabrication of miniaturized microfluidic paper-based analytical devices for sandwich enzyme-linked immunosorbent assays using INKJET printing.

Appl Biochem Microbiol 57:257–261. https://doi.org/10.1134/s0003683821020071

Lee YH, Wong DT (2009) Saliva: an emerging biofluid for early detection of diseases. Am J Dent 22:241–248

Lei KF, Huang CH, Kuo RL, Chang CK, Chen KF, Tsao KC, Tsang NM (2015) Paper-based enzyme-free immunoassay for rapid detection and subtyping of influenza A H1N1 and H3N2 viruses. Anal Chim Acta 883:37–44. https://doi.org/10.1016/j.aca.2015.02.071

Lewis GG, DiTucci MJ, Baker MS, Phillips ST (2012) High throughput method for prototyping three-dimensional, paper-based microfluidic devices. Lab Chip 12:2630–2633. https://doi.org/10.1039/c2lc40331e

Li X, Liu X (2014) Fabrication of three-dimensional microfluidic channels in a single layer of cellulose paper. Microfluid Nanofluid 16:819–827. https://doi.org/10.1007/s10404-014-1340-z

Li X, Tian J, Nguyen T, Shen W (2008) Paper-based microfluidic devices by plasma treatment. Anal Chem 80:9131–9134. https://doi.org/10.1021/ac801729t

Li X, Tian J, Garnier G, Shen W (2010) Fabrication of paper-based microfluidic sensors by printing. Colloids Surf B Biointerfaces 76:564–570. https://doi.org/10.1016/j.colsurfb.2009.12.023

Li F, Liu J, Guo L, Wang J, Zhang K, He J, Cui H (2019) High-resolution temporally resolved chemiluminescence based on double-layered 3D microfluidic paper-based device for multiplexed analysis. Biosens Bioelectron 141:111472. https://doi.org/10.1016/j.bios.2019.111472

Li F, Guo L, Hu Y, Li Z, Liu J, He J, Cui H (2020) Multiplexed chemiluminescence determination of three acute myocardial infarction biomarkers based on microfluidic paper-based immunodevice dual amplified by multifunctionalized gold nanoparticles. Talanta 207:120346. https://doi.org/10.1016/j.talanta.2019.120346

Lin D, Li B, Qi J, Ji X, Yang S, Wang W, Chen L (2020) Low cost fabrication of microfluidic paper-based analytical devices with water-based polyurethane acrylate and their application for bacterial detection. Sens Actuators B Chem. https://doi.org/10.1016/j.snb.2019.127213

Liu J, Kong X, Wang H, Zhang Y, Fan Y (2019) Roll-to-roll wax transfer for rapid and batch fabrication of paper-based microfluidics. Microfluid Nanofluid. https://doi.org/10.1007/s10404-019-2310-2

Ma L, Nilghaz A, Choi JR, Liu X, Lu X (2018) Rapid detection of clenbuterol in milk using microfluidic paper-based ELISA. Food Chem 246:437–441. https://doi.org/10.1016/j.foodchem.2017.12.022

Määttänen A, Fors D, Wang S, Valtakari D, Ihalainen P, Peltonen J (2011) Paper-based planar reaction arrays for printed diagnostics. Sens Actuators B Chem 160:1404–1412. https://doi.org/10.1016/j.snb.2011.09.086

Maejima K, Tomikawa S, Suzuki K, Citterio D (2013) Inkjet printing: an integrated and green chemical approach to microfluidic paper-based analytical devices. RSC Adv. https://doi.org/10.1039/c3ra40828k

Manz A, Graber N, Widmer HM (1990) Miniaturized total chemical analysis systems: a novel concept for chemical sensing. Sens Actuators B Chem 1:244–248. https://doi.org/10.1016/0925-4005(90)80209-i

Martinez AW, Phillips ST, Butte MJ, Whitesides GM (2007) Patterned paper as a platform for inexpensive, low-volume, portable bioassays. Angew Chem Int Ed Engl 46:1318–1320. https://doi.org/10.1002/anie.200603817

Martinez AW, Phillips ST, Whitesides GM (2008a) Three-dimensional microfluidic devices fabricated in layered paper and tape. Proc Natl Acad Sci USA 105:19606–19611. https://doi.org/10.1073/pnas.0810903105

Martinez AW, Phillips ST, Wiley BJ, Gupta M, Whitesides GM (2008b) FLASH: a rapid method for prototyping paper-based microfluidic devices. Lab Chip 8:2146–2150. https://doi.org/10.1039/b811135a

Mathaweesansurn A, Thongrod S, Khongkaew P, Phechkrajang CM, Wilairat P, Choengchan N (2020) Simple and fast fabrication of microfluidic paper-based analytical device by contact stamping for multiple-point standard addition assay: application to direct analysis of urinary creatinine. Talanta 210:120675. https://doi.org/10.1016/j.talanta.2019.120675

Mercan Ö B, Kılıç V, Şen M (2021) Machine learning-based colorimetric determination of glucose in artificial saliva with different reagents using a smartphone coupled μPAD. Sensors and Actuators B: Chemical 329. https://doi.org/10.1016/j.snb.2020.129037

Mettakoonpitak J, Khongsoun K, Wongwan N, Kaewbutdee S, Siripinyanond A, Kuharuk A, Henry CS (2021) Simple biodegradable plastic screen-printing for microfluidic paper-based analytical devices. Sens Actuators B Chemical. https://doi.org/10.1016/j.snb.2021.129463

Modha S, Shen Y, Chamouni H, Mulchandani A, Tsutsui H (2021) Laser-etched grooves for rapid fluid delivery for a paper-based chemiresistive biosensor. Biosens Bioelectron 180:113090. https://doi.org/10.1016/j.bios.2021.113090

Nargang TM, Dierkes R, Bruchmann J et al (2018) Photolithographic structuring of soft, extremely foldable and autoclavable hydrophobic barriers in paper. Anal Methods 10:4028–4035. https://doi.org/10.1039/c8ay01010b

Nie J, Zhang Y, Lin L, Zhou C, Li S, Zhang L, Li J (2012) Low-cost fabrication of paper-based microfluidic devices by one-step plotting. Anal Chem 84:6331–6335. https://doi.org/10.1021/ac203496c

Nie J, Liang Y, Zhang Y, Le S, Li D, Zhang S (2013) One-step patterning of hollow microstructures in paper by laser cutting to create microfluidic analytical devices. Analyst 138:671–676. https://doi.org/10.1039/c2an36219h

Norouzi AR, Nikfarjam A, Hajghassem H (2018) PDMS–PMMA bonding improvement using SiO_2 intermediate layer and its application in fabricating gas micro valves. Microsyst Technol 24:2727–2736. https://doi.org/10.1007/s00542-017-3676-2

Olkkonen J, Lehtinen K, Erho T (2010) Flexographically printed fluidic structures in paper. Anal Chem 82:10246–10250. https://doi.org/10.1021/ac1027066

Osborn JL, Lutz B, Fu E, Kauffman P, Stevens DY, Yager P (2010) Microfluidics without pumps: reinventing the T-sensor and H-filter in paper networks. Lab Chip 10:2659–2665. https://doi.org/10.1039/c004821f

Park C, Han YD, Kim HV, Lee J, Yoon HC, Park S (2018) Double-sided 3D printing on paper towards mass production of three-dimensional paper-based microfluidic analytical devices (3D-muPADs). Lab Chip 18:1533–1538. https://doi.org/10.1039/c8lc00367j

Pena-Pereira F, Lavilla I, Bendicho C (2016) Paper-based analytical device for instrumental-free detection of thiocyanate in saliva as a biomarker of tobacco smoke exposure. Talanta 147:390–396. https://doi.org/10.1016/j.talanta.2015.10.013

Pesaran S, Rafatmah E, Hemmateenejad B (2021) An all-in-one solid state thin-layer potentiometric sensor and biosensor based on three-dimensional origami paper microfluidics. Biosensors (basel). https://doi.org/10.3390/bios11020044

Postulka N, Striegel A, Krausse M et al (2019) Combining wax printing with hot embossing for the design of geometrically well-defined microfluidic papers. ACS Appl Mater Interfaces 11:4578–4587. https://doi.org/10.1021/acsami.8b18133

Preechakasedkit P, Siangproh W, Khongchareonporn N, Ngamrojanavanich N, Chailapakul O (2018) Development of an automated wax-printed paper-based lateral flow device for alpha-fetoprotein enzyme-linked immunosorbent assay. Biosens Bioelectron 102:27–32. https://doi.org/10.1016/j.bios.2017.10.051

Puneeth SB, Salve M, Akshatha R, Goel S (2019) Realization of microfluidic paper-based analytical devices using a 3-d printer: characterization and optimization. IEEE Trans Device Mater Reliab 19:529–536. https://doi.org/10.1109/tdmr.2019.2927448

Pungjunun K, Yakoh A, Chaiyo S, Praphairaksit N, Siangproh W, Kalcher K, Chailapakul O (2021) Laser engraved microapillary pump paper-based microfluidic device for colorimetric and electrochemical detection of salivary thiocyanate. Mikrochim Acta 188:140. https://doi.org/10.1007/s00604-021-04793-2

Ramdzan AN, Almeida M, McCullough MJ, Kolev SD (2016) Development of a microfluidic paper-based analytical device for the determination of salivary aldehydes. Anal Chim Acta 919:47–54. https://doi.org/10.1016/j.aca.2016.03.030

Rattanarat P, Dungchai W, Cate DM, Siangproh W, Volckens J, Chailapakul O, Henry CS (2013) A microfluidic paper-based analytical device for rapid quantification of particulate chromium. Anal Chim Acta 800:50–55. https://doi.org/10.1016/j.aca.2013.09.008

Rossini EL, Milani MI, Carrilho E, Pezza L, Pezza HR (2018) Simultaneous determination of renal function biomarkers in urine using a validated paper-based microfluidic analytical device. Anal Chim Acta 997:16–23. https://doi.org/10.1016/j.aca.2017.10.018

Rossini EL, Milani MI, Lima LS, Pezza HR (2021) Paper microfluidic device using carbon dots to detect glucose and lactate in saliva samples. Spectrochim Acta A Mol Biomol Spectrosc 248:119285. https://doi.org/10.1016/j.saa.2020.119285

Ruecha N, Chailapakul O, Suzuki K, Citterio D (2017) Fully inkjet-printed paper-based potentiometric ion-sensing devices. Anal Chem 89:10608–10616. https://doi.org/10.1021/acs.analchem.7b03177

Sackmann EK, Fulton AL, Beebe DJ (2014) The present and future role of microfluidics in biomedical research. Nature 507:181–189. https://doi.org/10.1038/nature13118

Sameenoi Y, Nongkai PN, Nouanthavong S, Henry CS, Nacapricha D (2014) One-step polymer screen-printing for microfluidic paper-based analytical device (muPAD) fabrication. Analyst 139:6580–6588. https://doi.org/10.1039/c4an01624f

Santana-Jimenez LA, Marquez-Lucero A, Osuna V, Estrada-Moreno I, Dominguez RB (2018) Naked-eye detection of glucose in saliva with bienzymatic paper-based sensor. Sensors (basel). https://doi.org/10.3390/s18041071

Sechi D, Greer B, Johnson J, Hashemi N (2013) Three-dimensional paper-based microfluidic device for assays of protein and glucose in urine. Anal Chem 85:10733–10737. https://doi.org/10.1021/ac4014868

Shang Q, Zhang P, Li H, Liu R, Zhang C (2019) A flow chemiluminescence paper-based microfluidic device for detection of chromium (III) in water. J Innov Opt Health Sci. https://doi.org/10.1142/s1793545819500160

Sitanurak J, Fukana N, Wongpakdee T, Thepchuay Y, Ratanawimarnwong N, Amornsakchai T, Nacapricha D (2019) T-shirt ink for one-step screen-printing of hydrophobic barriers for 2D- and 3D-microfluidic paper-based analytical devices. Talanta 205:120113. https://doi.org/10.1016/j.talanta.2019.120113

Sones CL, Katis IN, He PJ et al (2014) Laser-induced photo-polymerisation for creation of paper-based fluidic devices. Lab Chip 14:4567–4574. https://doi.org/10.1039/c4lc00850b

Songjaroen T, Dungchai W, Chailapakul O, Laiwattanapaisal W (2011) Novel, simple and low-cost alternative method for fabrication of paper-based microfluidics by wax dipping. Talanta 85:2587–2593. https://doi.org/10.1016/j.talanta.2011.08.024

Songjaroen T, Dungchai W, Chailapakul O, Henry CS, Laiwattana-paisal W (2012) Blood separation on microfluidic paper-based analytical devices. Lab Chip 12:3392–3398. https://doi.org/10.1039/c2lc21299d

Songok J, Tuominen M, Teisala H, Haapanen J, Makela J, Kuusipalo J, Toivakka M (2014) Paper-based microfluidics: fabrication technique and dynamics of capillary-driven surface flow. ACS Appl Mater Interfaces 6:20060–20066. https://doi.org/10.1021/am5055806

Soum V, Kim Y, Park S et al (2019) Affordable fabrication of conductive electrodes and dielectric films for a paper-based digital microfluidic chip. Micromachines (basel). https://doi.org/10.3390/mi10020109

Sun S, Wang Y, Ming T et al (2021) An origami paper-based nanoformulated immunosensor detects picograms of VEGF-C per milliliter of blood. Commun Biol 4:121. https://doi.org/10.1038/s42003-020-01607-8

Tang R, Yang H, Choi JR et al (2017) Paper-based device with on-chip reagent storage for rapid extraction of DNA from biological samples. Microchim Acta 184:2141–2150. https://doi.org/10.1007/s00604-017-2225-0

Teepoo S, Arsawiset S, Chanayota P (2019) One-step polylactic acid screen-printing microfluidic paper-based analytical device: application for simultaneous detection of nitrite and nitrate in food samples. Chemosensors. https://doi.org/10.3390/chemosensors7030044

Tiwari M (2011) Science behind human saliva. J Nat Sci Biol Med 2:53–58. https://doi.org/10.4103/0976-9668.82322

Trofimchuk E, Hu Y, Nilghaz A, Hua MZ, Sun S, Lu X (2020) Development of paper-based microfluidic device for the determination of nitrite in meat. Food Chem 316:126396. https://doi.org/10.1016/j.foodchem.2020.126396

Vella SJ, Beattie P, Cademartiri R et al (2012) Measuring markers of liver function using a micropatterned paper device designed for blood from a fingerstick. Anal Chem 84:2883–2891. https://doi.org/10.1021/ac203434x

Wang S, Ge L, Song X, Yu J, Ge S, Huang J, Zeng F (2012) Paper-based chemiluminescence ELISA: lab-on-paper based on chitosan modified paper device and wax-screen-printing. Biosens Bioelectron 31:212–218. https://doi.org/10.1016/j.bios.2011.10.019

Washburn EW (1921) The dynamics of capillary flow. Phys Rev 17:273–283. https://doi.org/10.1103/PhysRev.17.273

Wei X, Guo J, Lian H, Sun X, Liu B (2021) Cobalt metal-organic framework modified carbon cloth/paper hybrid electrochemical button-sensor for nonenzymatic glucose diagnostics. Sens Actu B Chem 329:129205. https://doi.org/10.1016/j.snb.2020.129205

Whitaker S (1986) Flow in porous media I: a theoretical derivation of Darcy's law. Transp Porous Media 1:3–25. https://doi.org/10.1007/BF01036523

Xiao W, Gao Y, Zhang Y, Li J, Liu Z, Nie J, Li J (2019) Enhanced 3D paper-based devices with a personal glucose meter for highly sensitive and portable biosensing of silver ion. Biosens Bioelectron 137:154–160. https://doi.org/10.1016/j.bios.2019.05.003

Yang X, Forouzan O, Brown TP, Shevkoplyas SS (2012) Integrated separation of blood plasma from whole blood for microfluidic paper-based analytical devices. Lab Chip 12:274–280. https://doi.org/10.1039/c1lc20803a

Yao X, Jia T, Xie C, Fu J, He Y (2016) Facial fabrication of paper-based flexible electronics with flash foam stamp lithography. Microsyst Technol 23:4419–4426. https://doi.org/10.1007/s00542-016-3207-6

Yehia AM, Farag MA, Tantawy MA (2020) A novel trimodal system on a paper-based microfluidic device for on-site detection of the date rape drug "ketamine." Anal Chim Acta 1104:95–104. https://doi.org/10.1016/j.aca.2020.01.002

Yu P, Deng M, Yang Y, Nie B, Zhao S (2020) 3D microfluidic devices in a single piece of paper for the simultaneous determination of nitrite and thiocyanate. Sensors (basel). https://doi.org/10.3390/s20154118

Zhang Y, Bai J, Ying JY (2015) A stacking flow immunoassay for the detection of dengue-specific immunoglobulins in salivary fluid. Lab Chip 15:1465–1471. https://doi.org/10.1039/c4lc01127a

Zhang Y, Liu J, Wang H, Fan Y (2019) Laser-induced selective wax reflow for paper-based microfluidics. RSC Adv 9:11460–11464. https://doi.org/10.1039/c9ra00610a

Zheng X, Zhang F, Wang K et al (2021) Smart biosensors and intelligent devices for salivary biomarker detection. TrAC Trends Anal Chem. https://doi.org/10.1016/j.trac.2021.116281